Linear plane wave propagation and normal transmission and reflection at discontinuity surfaces in second gradient 3D Continua

Francesco Dell'Isola, Angela Madeo, Luca Placidi

Zeitschrift für Angewandte Mathematik und Mechanik, 6 June 2011

Linear plane wave propagation and normal transmission and reflection at discontinuity surfaces in second gradient 3D Continua

Francesco dell'Isola[1,4,5*], **Angela Madeo**[2,5 **], **and Luca Placidi**[3,4,5***]

[1] Dipartimento di Ingegneria Strutturale e Geotecnica, Università di Roma La Sapienza, Via Eudossiana 18, 00184, Roma, Italy

[2] Laboratoire de Génie Civil et Ingénierie Environnementale, Université de Lyon–INSA, Bâtiment Coulomb, 69621 Villeurbanne Cedex, France

[3] Università Telematica Internazionale Uninettuno, Corso V. Emanuele II 39, 00186 Roma Italy

[4] Laboratorio Strutture e Materiali Intelligenti, Fondazione Tullio Levi-Civita, Via S. Pasquale snc, Cisterna di Latina, Italy

[5] International Center M&MOCS "Mathematics and Mechanics of Complex Systems", Palazzo Caetani, Cisterna di Latina, Italy

Received XXXX, revised XXXX, accepted XXXX
Published online XXXX

Key words Second gradient solids, Compression waves, Reflection and transmission at discontinuity surfaces, Indirect measurements

MSC (2000) 04A25

We study plane waves in second gradient solids and their reflection and transmission at plane displacement discontinuity surfaces. The needed extension of the treatment adopted to study plane wave propagation in Cauchy continua is not straightforward and is developed here. In particular, the balance of mechanical energy valid for second gradient continua is deduced. The presented results may be of interest as many boundary layer phenomena can be accounted for by second gradient models. We prove that second gradient elastic moduli may influence, in a measurable manner, how planar waves behave at discontinuity surfaces: the novel results presented here can be the basis of experimental procedures to estimate some among these moduli. We explicitly remark that reflection and transmission coefficients which we have estimated show a significant dependence on frequency, which indeed makes easier to conceive effective measurement methods.

1 Introduction

In [45], [44] and [46] a complete and consistent continuum theory allowing for the dependence of deformation energy on second gradient of placement is presented, which systematizes a series of results presented in [47], [48], [49], [96], [97], [70], [71], [72] [16] and [17]. Second gradient continuum theory does not fit Cauchy format for continuum mechanics. For this reason, only recently the it was appreciated (see [34]). Second gradient constitutive equations have been recognized to be essential in describing interface phenomena in phase-transition (see e.g. [25], [18], [88], [89]). More recently, second gradient constitutive equations are being considered of interest also for solids (see, among many others, e.g. [52], [95], [94], [69], [100], [3], [54], [55], [57], [59], [56], [58], [101]), [93]. Second gradient continua are a particular instance of multipolar continua, often also called higher order continua, in which the state of deformation is described by the first $n-order$ gradients of displacement and consequently the state of stress has to be modelled by means of n independent stress tensors (see [47], [48], [49]). Moreover the differential equations which govern the evolution of multipolar continua are of higher order and need boundary conditions more complicated than those used in Cauchy continuum models. Especially this circumstance caused many controversies and discussions about the physical meaning of the various kind of boundary conditions which were proposed (see e.g. [9]).

* e-mail: francesco.dellisola@uniroma1.it
** Corresponding author, e-mail: angela.madeo@insa-lyon.fr, Phone: +33 (0) 4 72 43 84 63
*** e-mail: luca.placidi@uniroma1.it

1.1 Second gradient Continua are a non-trivial generalization of Cauchy Continua

Many investigators refused to consider the generalizations proposed in [47], [48], [49], [96], [97], [70], [71] [16]and [17] until Germain framed clearly second gradient models in the format given to continuum mechanics by Cosserat brothers in their fundamental works ([20], [21]). This format was -since then- widely accepted (see e.g. [8]) and starts from the Principle of Least Action or from the Principle of Virtual Works and has been more recently been applied in different contexts (see e.g. [63], [64], [65], [23], [24], [40] and [41].

Let B be the body the motion of which needs to be described and let S_B be a regular sub-body of B: following the ideas already presented in [21], Germain assumes that the external powers balance the internal powers plus inertial powers for every S_B. A very elegant textbook which bases continuum mechanics on such a treatment is [87], while an accurate and updated review of the available results in this research field is given in [66]. When there exists a deformation energy, then the internal power can be represented as its first variation. When the system is conservative, the postulated principle of virtual works reduces to the assumption that the action functional is stationary. On the other hand, it is possible, by means of a Hamilton-Rayleigh principle (see e.g. [32]), to deduce a particular form of the principle of virtual works from a given action and Rayleigh dissipation functionals.

It has to be explicitly remarked that Germain's (and multipolar continuum) theory does not fit Cauchy format for continuum mechanics (although not all authors seems to be aware of this circumstance: see e.g. [36]). Indeed, so-called Cauchy postulate for contact actions is seen to hold, actually, only for a class of materials which results to be rather particular. Indeed, it results that Cauchy postulate is actually the restriction on the set of constitutive equations which characterizes Cauchy continua. It has been known since long time (see e.g. [17]) that when deformation energy depends on second gradient of displacement then contact surface force densities at every Cauchy cut must, in general, depend on the curvature of such Cauchy cut. Only in very particular cases (see e.g. [31]) second gradient continua show contact actions which may somehow reduce to the type described by Cauchy. Dependence of contact forces on curvature implies that also contact edge forces must be present: this circumstance needed the development of many sophisticated mathematical considerations and theories (see [81], [31], [6], [27], [28], [60], [67], [68], [91], [92], [52]).

By means of Cauchy stress tensor only it is not possible to describe the more complex contact interactions occurring in second gradient continua. Indeed, contact surface force densities depending on curvature of Cauchy cuts must arise together with i) contact double-force surface densities and ii) contact edge line force densities. Contact double-forces (of which contact couples are a particular case) expend power on normal velocity gradients through Cauchy cuts and contact edge line density forces arise at those lines on Cauchy cuts where the normal suffers concentrated discontinuities. This point is thoroughly investigated in the literature: for more details we refer e.g. to [81], [31] and all the references there cited. Therefore the structure of contact interactions in second gradient continua is much more complicated than in the case of Cauchy continua and needs a more complex mathematical formulation.

Second gradient constitutive equations have been widely recognized to be essential in describing interface phenomena in phase-transition. Indeed, at the interface between different fluid phases, contact actions are not, because of long range molecular interactions, falling in the theoretical framework established by Cauchy. This circumstance has been recognized already by de [25] (see also [90], [18], [42], [43], [30], [29] and references there cited).

More recently also second gradient constitutive equations for solids and porous media are being considered of interest. The number of papers describing second gradient models is increasing. For models describing phenomena occurring in fluid saturated porous media we cite: [19], [32], [86], [85] and [61]. For applications to plasticity and damage we limit ourselves to cite: [98], [39], [4], [2], [84].

Finally, we remark that many efforts were directed to identify microscopic structures which, when modelled at a macroscopic level by means of continuum mechanics, need the introduction of second or higher gradient theories: we limit ourselves to cite [99], [100], [7], [1], [5], [53], [83], [38]. For applications of micro-macro identification methods to phenomena in granular materials we have found interesting the approach used in [101] and [102], and [80].

One has to remark explicitly here that, in the present paper, we have refrained from considering phenomena in which a relevant amount of kinetic energy can be associated to "microscopic" degrees of freedom: therefore in the expression of kinetic energy we have not included any time derivative of strain gradient. It has to be underlined that (see [14], [13], [**?**], [10]) many interesting phenomena may occur when in a mechanical system "macroscopic" degrees of freedom are coupled with a large amount of "microscopic" degrees of freedom having "many" and "suitably distributed" natural vibration frequencies. In order to account for some of these phenomena a "macroscopic" damping term may be added (for instance using a Rayleigh-Hamilton approach) to the evolution second gradient equations.

1.2 Well-posed Boundary Conditions and the physical meaning of second gradient theories.

Many controversies which arose in the past about the importance and use of second gradient models concerned the physical interpretation of the required boundary conditions and the need of establishing measurement procedures for second gradient constitutive parameters.

The first issue arises whenever a novel theory is introduced by means of the least action principle or by means of Hamilton-Rayleigh principle or by means of the principle of virtual work. The needed interpretation of the obtained boundary conditions has been, in our opinion, satisfactorily given by Germain, Green, Rivlin, Toupin and Mindlin. It has to be clearly remarked (although this statement may be considered obvious) that boundary conditions obtained by means of a Least Action Principle or a Principle of Virtual Works are easily seen to be mathematically well-posed, once suitable assumptions are accepted on deformation and dissipation energy functionals.

In this paper, we propose to address the second issue (i.e. how to determine experimentally some of the introduced second gradient constitutive parameters): to do so we study plane waves in second gradient solids and their reflection and transmission at planar surfaces in which displacement and/or its normal derivative may suffer a jump. Our aim is to start, for second gradient solids, to generalize the classical study of wave propagation which, for standard first gradient elastic media, is presented in many textbooks. We found particularly interesting -among those more often used- [50] and [51]. This extension is feasible but non-trivial: for instance we needed to extend the treatment due to [18] to second gradient solids. In quoted paper the mechanical energy balance for second gradient fluids is established in Eulerian description. We extend it to second gradient solids by using a Lagrangian description.

About the important question concerning the phenomena which may be described by means of second gradient models there is a rather widespread agreement in the literature: many interesting boundary layer phenomena, related to the underlying micro-structure, can be accounted for by means of these models and these boundary phenomena may greatly influence wave propagation, transmission and reflection. To our knowledge, only in [96] such a theoretical study has been initiated, even if only for a particular class of second gradient continua: those for which double contact forces reduce to contact couples. Toupin studies accurately how dispersion formulas change when considering second gradient continua: with few modifications we can use his results as they are. However, we needed to prove that second gradient constitutive parameters determine, in a measurable manner, how planar waves behave at considered discontinuity surfaces. The novel results presented here can be the basis of experimental procedures to estimate some of second gradient constitutive parameters. Indeed, we show that for some kinds of boundary conditions the reflection and transmission coefficients remarkably depend on second gradient elastic moduli and that this dependence is increased when the frequency of the incident wave increases. We also showed the influence of second gradient elastic moduli on the dependence on frequency of transmission and reflection coefficients and performed a preliminary comparison with some experimental results which have attracted our attention ([62]).

The principal aim of this paper is to explicitly show how second gradient theories allow for the description of frequency-dependent reflection and transmission phenomena at a discontinuity surface between two continua. Indeed, this dependence on frequency of the amount of transmitted/reflected energy is experimentally often observed (see e.g. [37]) and is related on particular physical phenomena occurring in the medium due to the interaction of the propagating wave with an underlying micro-structure. Indeed, experience shows that many characteristics of reflected/transmitted waves often depend on the frequency of the incident wave. Nevertheless, this dependence is not taken into account by classical continuum models. A second gradient theory, on the other hand, allows for the possibility of describing some of the observed frequency-dependent phenomena since it is capable of taking into account the existence of a micro-structure at smaller scale, while classical Cauchy continuum theory is based on the hypothesis that the medium which it describes is completely homogeneous at microscopic level, i.e. that any kind of heterogeneity is present inside a Representative Elementary Volume of the continuum matrix. On the contrary, as in reality a perfectly continuum medium does not exist, all media are heterogeneous at a sufficiently small scale. If the wavelength of the travelling wave is comparable to the characteristic length of the underlying micro-structure (e.g. spacing between the heterogeneities at the micro-scale) then the propagation phenomena will be consistently affected by the presence of these heterogeneities. Instead, if the wavelength is sufficiently bigger than this characteristic length then the medium will behave rather as a continuum and the propagation phenomena will be poorly affected by the presence of a heterogeneous micro-structure. These expected frequency-dependent phenomena related to the presence of a heterogeneous micro-structure are forecast by our model and are carefully discussed in the section 6 of this paper.

On the other hand, the problem of extending the presented results to the case of non-orthogonal plane waves and to more general boundary conditions including surface mechanical properties of the interface and to wave propagation in second gradient porous media will be addressed in future investigations. Further generalization should also include the study of propagation of waves in non-linear/non-isotropic second gradient continua. This could be done generalizing the results presented e.g. in [35], where some interesting results on wave propagation in pre-stressed anisotropic media are presented.

1.3 Applicability of presented theoretical treatment and the possibility of considering more complex boundary conditions.

First of all we must remark that, although second gradients of displacement are introduced in the proposed model, it remains linear when considering its application to wave propagation. This means that, in the presented treatment, we can continue to use the so called "principle of superposition of effects". We are aware of the fact that real waves are not monochromatic: however reasonably "narrow" Fourier spectra are experimentally feasible when producing acoustic waves (see e.g. [62]).

Secondly we are also aware that at the interface of different solids many phenomena may occur: related to sharp variations of elastic moduli, imperfections, non-perfect adhesion and so on. Interfaces may be sharp or may have a thickness of the order of magnitude of the wavelength. Moreover, the interfaces may be endowed with mass, deformation energy, frictional properties and other physical properties. Many investigations has been made in this field: we consider very interesting those presented in [73] or in [75], [76], [77], [78], [80] which suggest how in our model one could incorporate micromechanical, frictional effects or interfacial roughness and nonlinearities. Moreover, if some uncertainties or inhomogeneities are present at a "microscopic" level in the neighborhood of the interface then the methods developed in [12] or [22] would allow the formulation of suitable "interface balance of energy" by generalizing the condition formulated in the present paper: the methods presented in cited papers seem most suitable as they are capable to account for nonstationary processes also .

Using the Archimedean spirit we would like to focus our attention only to those phenomena which may be described by second gradient models: a good experimental setup has to be conceived to isolate (exactly!) the phenomena which presented model can describe distinguishing them from all the others. One has to be aware that there are left (as it always happens!) relevant phenomena which we refrain from modelling here. Indeed, this is exactly the most suitable approach to be used: introducing too complex models could imply the need of very complicated numerical simulations (see e.g. the efforts needed in [79] to attack what is a rather simplified model of contact phenomena).

In second gradient continua two kinds of contact actions are possible: they correspond, at a microscopic level, to shorter range and longer range interactions. These two kind of contact interactions are related to two different kinds of macroscopic deformation energies: depending respectively on strain and strain gradient.

Longer range (or second gradient) interactions may be the source of boundary layers at discontinuity surfaces. We want to understand how to detect these boundary layers by means of measurements of the intensity of transmitted and reflected monochromatic waves. Therefore we assume that it is possible i) to prepare an interface thin enough and ii) to send towards it a monochromatic plane wave having a wavelength greater than the interface thickness but comparable with the range of long interactions.

We consider few boundary conditions which arise naturally in the framework of the theory of second gradient continua. One of these boundary conditions is based on the assumption that at the transmitting and reflecting interface the displacements of the two half spaces are arbitrary and that the mechanical connection between them is assured only by "long range" (second gradient) contact actions: in the remainder of this paper we will call this constraint "generalized internal roller". Such an assumption can account for an interface which has been "weakened" with respect to the "undamaged" solids which it is connecting: it is clearly valid only when these displacement are small enough. When displacements are large or when the solids in contact are porous and infused by a fluid then shock waves may be initiated and more generally impact phenomena can be of relevance at the interface: in these case the study presented in Carcaterra*et al*. (2000) and Carcaterra and Ciappi (2000) may indicate some useful generalizations of the boundary conditions which we present here.

In conclusion: the present paper wants to establish some theoretical predictions which are valid under all previously listed assumptions. This seems to be reasonable and experimental setups described by the presented model seem physically feasible. Indeed the preliminary comparison with some experimental data which we could find in the literature ([62]) shows that the dependence of reflected wave intensity on frequency which we forecast is, at least qualitatively, similar to those they measured .

2 Mechanical energy transport in second gradient continua

In this section we deduce, starting from the appropriate equation of motion, the mechanical energy conservation law for a three-dimensional second gradient continuum. Similar results can be found in [18] for second gradient fluids.

Let $\chi : B \times (0,T) \to \mathbb{R}^3$ be the placement map which, at any instant t, associates to any material particle $\mathbf{X} \in B$ its position in the physical space. The displacement field is then defined as $\mathbf{u}(\mathbf{X},t) := \chi(\mathbf{X},t) - \mathbf{X}$. We set $\mathbf{F} := \nabla\chi$ and we denote by $\boldsymbol{\varepsilon} := (\mathbf{F}^T \cdot \mathbf{F} - \mathbf{I})/2$ the classical Green-Lagrange deformation tensor. Let ρ be the mass per unit volume of the considered continuum in its reference configuration, we introduce, by means of

$$\mathcal{E} = \frac{1}{2}\rho\left(\dot{\mathbf{u}}\right)^2 + \Psi\left(\boldsymbol{\varepsilon}, \nabla\boldsymbol{\varepsilon}\right), \tag{1}$$

the total Lagrangian energy density of the considered second gradient continuum, as given by the sum of the kinetic and deformation energy, which we denote by Ψ. Here and in the sequel a superposed dot represents partial differentiation with respect to time, i.e. what is usually called the material time derivative. Moreover, we recall that, in absence of body forces, the equation of motion for a second gradient continuum reads (see e.g. [45], [33] or [86] for a variational deduction of the equations of motion for second gradient materials) [1]

$$div\left[\mathbf{F}\cdot\left(\frac{\partial\Psi}{\partial\boldsymbol{\varepsilon}}-div\left(\frac{\partial\Psi}{\partial\nabla\boldsymbol{\varepsilon}}\right)\right)\right]=\rho\ddot{\mathbf{u}} \tag{2}$$

Differentiating Eq. (1) with respect to time and using Eq. (2), it can be shown that [2]

$$\frac{\partial\mathcal{E}}{\partial t}+div\left[-\dot{\mathbf{u}}\cdot\mathbf{F}\cdot\left(\frac{\partial\Psi}{\partial\boldsymbol{\varepsilon}}-div\left(\frac{\partial\Psi}{\partial\nabla\boldsymbol{\varepsilon}}\right)\right)-\left((\nabla\dot{\mathbf{u}})^{T}\cdot\mathbf{F}\right):\frac{\partial\Psi}{\partial\nabla\boldsymbol{\varepsilon}}\right]=0. \tag{3}$$

In the calculations for obtaining Eq. (3) we used the fact that $\boldsymbol{\varepsilon}$ is a second order symmetric tensor, that $\nabla\boldsymbol{\varepsilon}$ is a third order tensor symmetric with respect to its first two indices and that $\nabla\mathbf{F}$ is a third order tensor symmetric with respect to its last two indices. Thus this last equation represents the Lagrangian form of energy balance for a second gradient 3D continuum in the general non-linear case.

We now want to focus our attention to the particular case of linear elasticity in order to study linear plane waves in second gradient 3D continua. To this purpose, we note that, when linearising in the neighbourhood of a stress-free reference configuration, the gradient of placement $\mathbf{F}$ in Eq. (3) is substituted by the identity matrix and that the equation of motion and mechanical energy balance for a second gradient continuum respectively reduce to

$$div\left[\mathbf{S}-div\mathbf{P}\right]=\rho\ddot{\mathbf{u}},\qquad\frac{\partial\mathcal{E}}{\partial t}+div\left[-\dot{\mathbf{u}}\cdot(\mathbf{S}-div\mathbf{P})-(\nabla\dot{\mathbf{u}})^{T}:\mathbf{P}\right]=0, \tag{4}$$

where, following the nomenclature of Germain, $\mathbf{S}$ and $\mathbf{P}$ are the linearised Piola-Kirchoff first and second gradient stress tensors respectively. In order to lighten the notation, however, we will refer to these two tensors simply as stress and hyper-stress tensor respectively. It is well known that in the case of isotropic material $\mathbf{S}=2\,\mu\,\mathbf{E}+\lambda\,(tr\mathbf{E})\,\mathbf{I}$, where $\mathbf{E}=(\nabla\mathbf{u}+(\nabla\mathbf{u})^{T})/2$ is the linearised Green-Lagrange deformation tensor and λ and μ are the so-called Lamé coefficients. As for the hyper-stress third order tensor $\mathbf{P}$, it can be shown (see e.g. [**?**]DSV that in the case of isotropic materials it takes the following simplified form[3]

$$\begin{aligned}\mathbf{P}=&c_2\left[2\mathbf{I}\otimes div\mathbf{E}+(\mathbf{I}\otimes\nabla(tr\mathbf{E}))^{T_{23}}+\nabla(tr\mathbf{E})\otimes\mathbf{I}\right]+c_3\mathbf{I}\otimes\nabla(tr\mathbf{E})\\&+2c_5\left[(\mathbf{I}\otimes div\mathbf{E})^{T_{23}}+div\mathbf{E}\otimes\mathbf{I}\right]+2c_{11}\nabla\mathbf{E}+4c_{15}(\nabla\mathbf{E})^{T_{12}},\end{aligned} \tag{5}$$

where c_2, c_3, c_5, c_{11} and c_{15} are constants depending on the material properties of the considered second gradient continuum. As it will be seen to be useful later on, we define the following coefficients

$$\Lambda:=c_3+2(c_5+c_{15})+4c_2,\qquad M:=c_{11}+c_{15}+c_5, \tag{6}$$

which parallel the first gradient Lamé coefficients λ and μ.

3 Dispersion Formulas

Let us now consider a wave travelling in the considered second gradient continuum. We denote by x_1 the axis of a reference frame the direction of which coincides with the propagation direction and by x_2 and x_3 the other two directions forming a Cartesian basis with x_1. We assume that the displacement vector has three non-vanishing components depending only on the x_1 coordinate and on time, i.e. $\mathbf{u}(x_1,t)=(u_1(x_1,t),u_2(x_1,t),u_3(x_1,t))$. In the following we will say that we are in

[1] The symbol div stands for the usual divergence operator, e.g. $(div\mathbf{A})_{ij}=\mathbf{A}_{ijk,k}$. Here and in the sequel we adopt Einstein summation convention over repeated indices. The symbol ∇ stands for the usual gradient operator, e.g. $(\nabla\mathbf{A})_{ijk}=\mathbf{A}_{ij,k}$. A central dot indicates a simple contraction between two tensors of any order, e.g. $(\mathbf{A}\cdot\mathbf{B})_{ijhk}=\mathbf{A}_{ijp}\mathbf{B}_{phk}$

[2] A double dot indicates a double contraction between two tensors of any order, e.g. $(\mathbf{A}:\mathbf{B})_{ij}=\mathbf{A}_{ihk}\mathbf{B}_{khj}$.

[3] We define the transposition operations of a third order tensor as $A^{T_{23}}_{ijk}=A_{ikj}$ and $A^{T_{12}}_{ijk}=A_{jik}$ and the symbol $\otimes$ as the usual tensor product operation between two tensors of any order (e.g. $(A\otimes B)_{ijhk}=A_{ij}B_{hk}$)

presence of a unidirectional wave propagation. With this assumption it is easy to show that the associated matrix form of the linearised deformation tensor reads

$$\mathbf{E} = \begin{pmatrix} u_1' & u_2'/2 & u_3'/2 \\ u_2'/2 & 0 & 0 \\ u_3'/2 & 0 & 0 \end{pmatrix} \tag{7}$$

where we clearly denote by an apex the partial differentiation with respect to the space variable x_1. Using (7) to calculate the stress and hyper-stress tensors $\mathbf{S} = 2\mu\mathbf{E} + \lambda(tr\mathbf{E})\,\mathbf{I}$ and $\mathbf{P}$ (see Eqs. (5) and (6)), the equation of motion $(4)_1$ takes the following form

$$(\lambda + 2\mu)u_1'' - (\Lambda + 2M)u_1'''' = \rho\ddot{u}_1, \tag{8}$$

$$\mu u_2'' - M u_2'''' = \rho\ddot{u}_2, \qquad \mu u_3'' - M u_3'''' = \rho\ddot{u}_3. \tag{9}$$

We notice that the equations of motion obtained in this unidirectional wave propagation are completely uncoupled due to the particular constitutive relations assumed for isotropic, linear elastic, second gradient continua. Moreover, the conservation of energy $(4)_2$ gives $\partial\mathcal{E}/\partial t + H' = 0$ where we denote

$$\begin{aligned} H := &-(\lambda + 2\mu)(u_1'\dot{u}_1) - \mu(u_2'\dot{u}_2) - \mu(u_3'\dot{u}_3) \\ &+ (\Lambda + 2M)(u_1'''\dot{u}_1 - u_1''\dot{u}_1') + M(u_2'''\dot{u}_2 - u_2''\dot{u}_2') + M(u_3'''\dot{u}_3 - u_3''\dot{u}_3'), \end{aligned} \tag{10}$$

the energy flux in the considered particular case. We also remark that M and $\Lambda+2M$ are positive due to definite-positiveness of the internal energy (see e.g. dell'Isola *et al*. (2009b)). We now assume that the displacement field admits a classical wave solution in the form

$$\mathbf{u} = \begin{pmatrix} u_1 \\ u_2 \\ u_3 \end{pmatrix} = \begin{pmatrix} \alpha_1 \\ \alpha_2 \\ \alpha_3 \end{pmatrix} e^{i(\omega t - k x_1)} \tag{11}$$

where the eigenvector $(\alpha_1, \alpha_2, \alpha_3)$ gives the longitudinal and transversal amplitudes of the considered wave, ω is the positive real frequency and k its wave number. Using this wave form for $\mathbf{u}$ in the equations of motion for longitudinal and transversal displacement (8) and (9) we get the following dispersion relations for a second gradient continuum

$$(\Lambda + 2M)k_1^4 + (\lambda + 2\mu)k_1^2 - \rho\omega^2 = 0,$$

$$M k_2^4 + \mu k_2^2 - \rho\omega^2 = 0, \qquad M k_3^4 + \mu k_3^2 - \rho\omega^2 = 0,$$

where k_1 is the wave number relative to the eigenvector $(1,0,0)$, k_2 and k_3 are the wave numbers relative to the eigenvectors $(0,1,0)$ and $(0,0,1)$ respectively. Since we are dealing with isotropic media, the two transverse dispersion relations coincide: in what follows we therefore shall ignore the last dispersion relation.

Because of isotropy, the waves arising in considered medium can be either purely transversal or purely longitudinal. We now look for non-dimensional form of these relations by setting: $k_1 = k_l\tilde{k}_l, \omega = \omega_l\tilde{\omega}$ for longitudinal waves and $k_2 = k_t\tilde{k}_t$, $\omega = \omega_t\tilde{\omega}$ for transverse waves. Here k_l (or k_t), ω_l (or ω_t) are characteristic values of the wave number and of the frequency for longitudinal (or transverse) waves respectively; moreover, $\tilde{k}_l$, $\tilde{k}_t$ and $\tilde{\omega}$ are the corresponding dimensionless variables. This leads to

$$L_l^2 k_l^2 \tilde{k}_l^4 + \tilde{k}_l^2 - \frac{\rho}{(\lambda + 2\mu)}\frac{\omega_l^2}{k_l^2}\tilde{\omega}^2 = 0,$$

$$L_t^2 k_t^2 \tilde{k}_t^4 + \tilde{k}_t^2 - \frac{\rho}{\mu}\frac{\omega_t^2}{k_t^2}\tilde{\omega}^2 = 0,$$

where $L_l := \sqrt{(\Lambda + 2M)/(\lambda + 2\mu)}$ and $L_t := \sqrt{M/\mu}$ are the characteristic length of second gradient interactions for longitudinal and transversal waves respectively. To our knowledge, similar dispersion formulas for a particular class of second gradient materials has been already studied only by [96]. We finally choose k_l^2 and k_t^2 to be such that the coefficients of $\tilde{\omega}^2$ in the two dispersion relations are both equal to one and hence we get

$$k_l^2 = \rho\omega_l^2/(\lambda + 2\mu) \qquad k_t^2 = \rho\omega_t^2/\mu. \tag{12}$$

The dispersion relations thus reduce to

$$\epsilon_l^2 \tilde{k}_l^4 + \tilde{k}_l^2 - \tilde{\omega}^2 = 0, \qquad \epsilon_t^2 \tilde{k}_t^4 + \tilde{k}_t^2 - \tilde{\omega}^2 = 0, \tag{13}$$

where we set

$$\epsilon_l = k_l\, L_l, \qquad \epsilon_t = k_t\, L_t.$$

In other words, the introduced quantity ϵ_l (or ϵ_t) is the ratio between the characteristic second gradient length and the wave length for longitudinal (transverse) waves. The chosen non dimensional form of the dispersion equations implies that when $\tilde{\omega} = 1$, then the dimensional frequency ω takes the characteristic value $\omega = \omega_l = \epsilon_l L_l \sqrt{(\lambda + 2\mu)/\rho}$ in the case of longitudinal waves and the value $\omega = \omega_t = \epsilon_t L_t \sqrt{\mu/\rho}$ in the case of transverse waves. Analogously, when $\tilde{k} = 1$, then the dimensional wave number takes the characteristic value $k_1 = k_l = \epsilon_l / L_l$ in the case of longitudinal waves and the value $k_2 = k_t = \epsilon_t / L_t$ in the case of transverse waves.

The relationships between the dimensionless wave number and frequency is thus easily recovered both for longitudinal and transverse waves by solving the bi-quadratic equations (13):

$$\tilde{k}_l = \pm\sqrt{\frac{-1 \pm \sqrt{1 + 4\,\epsilon_l^2\,\tilde{\omega}^2}}{2\epsilon_l^2}}, \qquad \tilde{k}_t = \pm\sqrt{\frac{-1 \pm \sqrt{1 + 4\,\epsilon_t^2\,\tilde{\omega}^2}}{2\epsilon_t^2}}.$$

If we consider the positive real numbers

$$\tilde{k}_l^p = \sqrt{\frac{-1 + \sqrt{1 + 4\,\epsilon_l^2\,\tilde{\omega}^2}}{2\epsilon_l^2}}, \qquad \tilde{k}_l^s = \sqrt{\frac{1 + \sqrt{1 + 4\,\epsilon_l^2\,\tilde{\omega}^2}}{2\epsilon_l^2}}, \tag{14}$$

$$\tilde{k}_t^p = \sqrt{\frac{-1 + \sqrt{1 + 4\,\epsilon_t^2\,\tilde{\omega}^2}}{2\epsilon_t^2}}, \qquad \tilde{k}_t^s = \sqrt{\frac{1 + \sqrt{1 + 4\,\epsilon_t^2\,\tilde{\omega}^2}}{2\epsilon_t^2}}, \tag{15}$$

the four roots associated to longitudinal waves are clearly $\pm\tilde{k}_l^p$, $\pm j\tilde{k}_l^s$, and analogously we have for the transverse waves the four roots $\pm\tilde{k}_t^p$, $\pm j\tilde{k}_t^s$, where j stands for the imaginary unit. It is clear that one can derive the corresponding dimensional quantities k_1^p and k_1^s (for longitudinal waves) and k_2^p and k_2^s (for transverse waves) just multiplying the non-dimensional roots $\tilde{k}_l$ and $\tilde{k}_t$ by k_l and k_t respectively (see eqs. (12)). As we will see in more detail later on, the roots $\tilde{k}^p$ are associated to *propagative waves* which are a second gradient generalization of the waves propagating in a first gradient material, while the roots $\tilde{k}^s$ are the so-called *standing waves* (or evanescent waves) (see e.g. [50], [51], [15]) and are peculiar of second gradient models. These standing waves will be seen to play a significant role close to material discontinuity surfaces in second gradient continua where phenomena of reflection and transmission may occur. Indeed, there are other physical situations in which standing waves may appear. For instance, [82] showed that this may occur when studying coupling between the transversal displacement u and the longitudinal displacement w in one-dimensional beams.

4 Natural and kinematical boundary conditions at surfaces where displacement or normal derivative of displacement may be discontinuous

The problem of finding boundary conditions to be imposed at discontinuity surfaces is always challenging for the modelling of any physical phenomenon. Indeed, the only possible method which leads to surely well-posed boundary conditions, compatible with the obtained bulk equations of motion, is to use a variational principle. This is the case also when looking for the correct set of boundary conditions associated to the motion of a second gradient continuum. We just recall here the boundary (or jump) conditions found for a second gradient material in dell'Isola [33] or [86]. The boundary conditions on the considered discontinuity surface S, in absence of external surface and line actions, can be deduced from the following duality conditions

$$[|\mathbf{t} \cdot \delta\mathbf{u}|] = 0, \qquad [|\boldsymbol{\tau} \cdot (\delta\mathbf{u})_n|] = 0, \qquad [|\mathbf{f} \cdot \delta\mathbf{u}\,|] = 0. \tag{16}$$

The first two of these conditions are valid on S while the last one is valid on the edges of S, if any. In the previous formulas (16) we set

$$\mathbf{t} := \left[\mathbf{F} \cdot \left(\frac{\partial \Psi}{\partial \boldsymbol{\varepsilon}} - div\left(\frac{\partial \Psi}{\partial \nabla \boldsymbol{\varepsilon}}\right)\right)\right] \cdot \mathbf{n} - div^S\left(\mathbf{F} \cdot \frac{\partial \Psi}{\partial \nabla \boldsymbol{\varepsilon}} \cdot \mathbf{n}\right),$$

$$\boldsymbol{\tau} := \left(\mathbf{F} \cdot \frac{\partial \Psi}{\partial \nabla \boldsymbol{\varepsilon}} \cdot \mathbf{n}\right) \cdot \mathbf{n}, \qquad \mathbf{f} := \left(\mathbf{F} \cdot \frac{\partial \Psi}{\partial \nabla \boldsymbol{\varepsilon}} \cdot \mathbf{n}\right) \cdot \boldsymbol{\nu}.$$

Moreover, $\mathbf{n}$ is the unit normal vector to the surface S, div^S stands for the surface divergence operator on S, if the edge is regarded as the border of a surface then $\boldsymbol{\nu}$ is the normal vector to the considered edge which is tangent to the surface, $\delta\mathbf{u}$ is the variation of the displacement field and $(\delta\mathbf{u})_n := \nabla(\delta\mathbf{u})\cdot\mathbf{n}$ stands for the normal derivative of the variation of the displacement field. Finally, given a quantity a defined everywhere and having continuous traces a^+ and a^-on the two sides of S respectively, we have set $[|a|] := a^+ - a^-$ (we use the same symbol for the jump across edges).

When choosing arbitrary displacement variation $\delta\mathbf{u}$ continuously varying through S and arbitrary normal derivative $(\delta\mathbf{u})_n$continuously varying through S in equations (16), one gets a particular set of *natural jump conditions*, which can be interpreted as the vanishing jump of internal surface forces ($[|\mathbf{t}|] = 0$), the vanishing jump of internal surface *double forces* ($[|\boldsymbol{\tau}|] = 0$) and the vanishing jump of internal line actions ($[|\mathbf{f}|] = 0$) respectively (see [45] and Germain (1973b) for the first introduction of the concept of contact double force). Indeed, if it happens that the displacement field, due to a particular constraint, verifies the particular equation $\delta\mathbf{u}^- = \delta\mathbf{u}^+ =: \delta\mathbf{u}$ (vanishing jump of the displacement field), and $\delta\mathbf{u}$ is arbitrary, then in order to fulfil conditions $(16)_1$ and $(16)_3$ one must require that also the jumps of the dual quantities to $\delta\mathbf{u}$ (i.e. surface forces and line forces) are vanishing. Analogously, if the normal derivative of displacement is assigned to be equal on both sides of S and this common value is arbitrary, then in order eq. $(16)_2$ to be verified one must also impose continuity of internal double forces. Conditions of the type $\delta\mathbf{u}^- = \delta\mathbf{u}^+$, or any similar relationship among $\delta\mathbf{u}^\pm$ and $(\delta\mathbf{u})_n^\pm$, are called *kinematical boundary conditions*. Once the kinematical boundary conditions are chosen, the associated dual conditions necessary and sufficient to fulfil duality conditions (16), are called natural boundary conditions associated to the chosen kinematical ones. Therefore, in addition to those previously discussed, other kinematical choices are possible in the previously formulated duality conditions, these choices being indicated by the admissible kinematics of the considered system or, in simpler words, by the considered phenomenology. We discuss here some kinematical constraints for second gradient continua, which we call *generalized internal clamp*, *generalized internal hinge* and *generalized internal roller* and the natural boundary conditions associated to them.

- *Generalized internal clamp*.

  We define this constraint imposing the continuity of both the displacement $\mathbf{u}$ and the normal derivative of displacement $\nabla\mathbf{u}\cdot\mathbf{n}$ (and therefore of the test function $\delta\mathbf{u}$ and of its normal derivative $(\delta\mathbf{u})_n$) at the discontinuity surface S which from now on we assume to be regular (i.e S has no edges). As already noticed, in this case boundary conditions are

$$[|\mathbf{u}\,|] = 0, \qquad [|\nabla\mathbf{u}\cdot\mathbf{n}|] = 0, \qquad [|\mathbf{t}|] = 0, \qquad [|\boldsymbol{\tau}|] = 0. \tag{17}$$

  If we consider unidirectional wave propagation, and if we choose a flat surface S such that its normal is given by $\mathbf{n} = (1,0,0)$, then the jump conditions (17) particularize into

$$\begin{aligned} &[|u_1|] = 0, \quad [|u_1'|] = 0, \quad [|(\lambda+2\mu)u_1' - (\Lambda+2M)u_1'''|] = 0, \quad [|(\Lambda+2M)u_1''|] = 0,\\ &[|u_2|] = 0, \quad [|u_2'|] = 0, \quad [|(\mu u_2' - Mu_2''')|] = 0, \quad [|Mu_2''|] = 0,\\ &[|u_3|] = 0, \quad [|u_3'|] = 0, \quad [|(\mu u_3' - Mu_3''')|] = 0, \quad [|Mu_3''|] = 0. \end{aligned} \tag{18}$$

- *Generalized internal elastic hinge*

  We introduce the constraint of generalized internal elastic hinge at surface S assuming that there exists a surface deformation energy density Ψ_S localized on S, quadratically dependent on the surface relative displacement. In other words, we assume that $\mathbf{u}^+$ and $\mathbf{u}^-$ can be different, and can vary independently. In formulas, the introduced surface deformation energy density is given by:

$$\Psi_S = \frac{1}{2}k_S^n(\mathbf{u}^+\cdot\mathbf{n} - \mathbf{u}^-\cdot\mathbf{n})^2 + \frac{1}{2}k_S^{\|}(u_{\|}^+ - u_{\|}^-)^2, \tag{19}$$

  where we denoted by $u_{\|}$ the tangential component of the displacement $\mathbf{u}$. When both surface elastic moduli k_S^n and $k_S^{\|}$ tend to infinity, this energy will impose continuity of displacements at S. We will assume that $(\delta\mathbf{u})_n^+$ and $(\delta\mathbf{u})_n^-$ can independently take arbitrary values on the two sides of S. These last conditions, together with the duality condition $(16)_2$, imply that the double forces must be separately vanishing on the two sides of S. In formulas, the four conditions for a generalized elastic hinge can be seen to read

$$[|\mathbf{t}|] = 0, \quad k_S^n\,[|\mathbf{u}\cdot\mathbf{n}\,|] = \mathbf{t}^+\cdot\mathbf{n}, \quad k_S^{\|}\,[|u_{\|}\,|] = t_{\|}^+, \quad \boldsymbol{\tau}^+ = 0, \quad \boldsymbol{\tau}^- = 0, \tag{20}$$

  where we denoted by $t_{\|}^+$ the tangential component of the force $\mathbf{t}^+$ on the $+$ side of S. More complex surface contact phenomena may be eventually modelled by means of more sophisticated boundary conditions. In this context future

investigations will exploit the results presented in [73], [75], [76], [78], [79]. In the considered unidirectional wave propagation these conditions reduce to

$$
\begin{aligned}
&[|(\lambda+2\mu)u_1' - (\Lambda+2M)u_1'''|] = 0, \qquad k_S^n\,[|u_1|] = ((\lambda+2\mu)u_1' - (\Lambda+2M)u_1''')^+, \\
&((\Lambda+2M)u_1'')^+ = 0, \qquad ((\Lambda+2M)u_1'')^- = 0 \\
&[|(\mu u_2' - Mu_2''')|] = 0, \qquad k_S^{\parallel}\,[|u_2|] = (\mu u_2' - Mu_2''')^+, \\
&(Mu_2'')^+ = 0, \qquad (Mu_2'')^- = 0, \\
&[|(\mu u_3' - Mu_3''')|] = 0, \qquad k_S^{\parallel}\,[|u_3|] = \mu u_3^{+\prime} - Mu_3^{+\prime\prime\prime} \\
&(Mu_3'')^+ = 0, \qquad (Mu_3'')^- = 0.
\end{aligned}
\tag{21}
$$

- *Generalized 3D internal roller*

  We define the last kind of kinematical constraint considered in this paper which we call generalized roller and which is defined in such a way that it allows independently arbitrary displacements on both sides of S (which implies separately $\delta\mathbf{u}^+$ and $\delta\mathbf{u}^-$ to be arbitrary) and such that the normal derivative of displacement is continuous through S (i.e. $[|\nabla\mathbf{u}\cdot\mathbf{n}|] = 0$). The first condition together with eq. $(16)_1$ implies that the generalized force must be separately vanishing on both sides of S, while the second condition implies continuity of double forces through S. Hence the four conditions for a generalized roller are

$$
\mathbf{t}^+ = 0, \qquad \mathbf{t}^- = 0, \qquad [|\nabla\mathbf{u}\cdot\mathbf{n}|] = 0, \qquad [|\boldsymbol{\tau}|] = 0. \tag{22}
$$

It can be shown that in the considered unidirectional propagation case these equations simplify into

$$
\begin{aligned}
&((\lambda+2\mu)u_1' - (\Lambda+2M)u_1''')^{\pm} = 0, \quad [|u_1'|] = 0, \quad [|(\Lambda+2M)u_1''|] = 0, \\
&(\mu u_2' - Mu_2''')^+ = (\mu u_2' - Mu_2''')^- = 0, \quad [|u_2'|] = 0, \quad [|Mu_2''|] = 0, \\
&(\mu u_3' - Mu_3''')^+ = (\mu u_3' - Mu_3''')^- = 0, \quad [|u_3'|] = 0, \quad [|Mu_3''|] = 0.
\end{aligned}
\tag{23}
$$

As occurs for the dispersion relations, also for the boundary conditions, we can notice that in the considered linear-elastic case, they are completely uncoupled in the longitudinal and transversal displacement due to isotropy and to the fact that the displacement only depends on the x_1 variable.

5 Transmission and reflection at discontinuity surfaces

Let us now recall that we are considering a flat discontinuity surface S inside the considered second gradient continuum. We denote by $\mathbf{n}$ the unit normal to S and we choose the fixed reference frame in such a way that $\mathbf{n}$ points in the x_1 direction: we are assuming that the vector $\mathbf{n}$ is always the same at any point of S (see Fig.1). As before, we denote by x_2 and x_3 the other two directions of the fixed reference frame forming a Cartesian basis with x_1. Using the equations of motion (8) and (9) on both sides of S and the linearised jump conditions (18), (21) or (23), we are able to describe the motion of two different isotropic, linear-elastic second gradient continua which are in contact through the discontinuity surface S and considering three different constraints at this surface (generalized internal clamp, generalized internal hinge and generalized internal roller). Nevertheless, in this paper we limit ourselves to the case of two second gradient continua with the same material properties (same first and second gradient elasticity parameters) in contact through the surface S at which we impose the three generalized types of constraints discussed before.

Let us start by studying the case of longitudinal waves (the involved field is then the one we previously denoted by u_1) impacting at the interface S and then we will repeat the reasoning for transverse waves (the involved field is then u_2): this is allowed to the fact that the obtained problem is completely uncoupled with respect to longitudinal and transversal displacements.

Then let us consider an incident longitudinal wave u_i^l propagating in the x_1 direction and defined as

$$
u_i^l = \alpha_i^l e^{j(\omega t - k_1^p x_1)},
$$

where α_i^l is the amplitude of the incident (subscript i), longitudinal (superscript l) wave which we assume to be assigned, ω is the real positive frequency of such an incident wave and, $k_1^p = \tilde{k}_l^p k_l$ (see eqs. $(14)_1$and 12) is the positive real wave

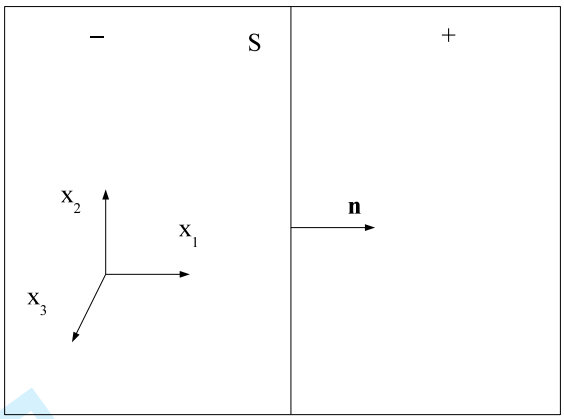

Fig. 1 Domain with flat discontinuity surface

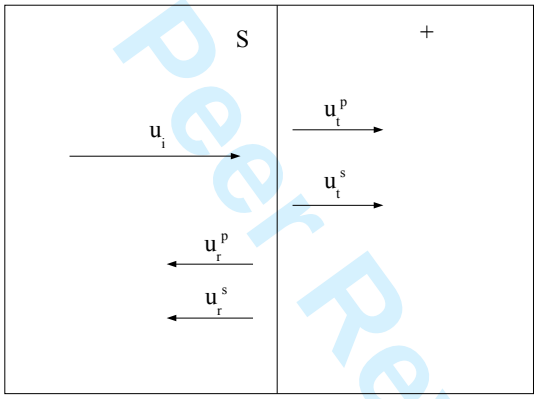

Fig. 2 Reflected and transmitted waves

number associated to the propagating wave travelling in the x_1 direction. When this wave reaches the interface S reflection and transmission phenomena take place (see Fig. 2). We call u_r^l and u_t^l the reflected and transmitted longitudinal wave respectively. According to the geometry of the considered problem and to equations (14) the reflected wave propagates always in the x_1 direction and take the following form

$$u_r^l = u_r^{lp} + u_r^{ls} = \alpha_r^l e^{j(\omega t + k_1^p x_1)} + \beta_r^l e^{j(\omega t - j k_1^s x_1)},$$

where α_r^l is the amplitude of the propagative reflected wave travelling in the $-x_1$ direction and β_r^l is the amplitude of the standing reflected wave. Note that $k_1^s = \tilde{k}_l^s k_l$ (see eqs. $(14)_2$ and (12)) is the positive real wave number associated to the standing wave and that the standing reflected wave vanishes as x_1 approaches $-\infty$. Analogously, the transmitted wave is may be represented by

$$u_t^l = u_t^{lp} + u_t^{ls} = \alpha_t^l e^{j(\omega t - k_1^p x_1)} + \beta_t^l e^{j(\omega t + j k_1^s x_1)},$$

where α_t^l is the amplitude of the propagative transmitted wave travelling in the x_1 direction and β_t^l is the amplitude of the standing transmitted wave. Note that the standing transmitted wave vanishes as x_1 approaches $+\infty$. We remark that, among the two possible standing reflected (transmitted) waves we did not consider that one which diverges as $x_1 \to -\infty$ ($x_1 \to +\infty$), as we assume a Sommerfeld-type condition at infinity.

As we want to deal with dimensionless quantities, we introduce the non-dimensional counterpart of these displacements by considering the non-dimensional variables $\tilde{t} = \omega_l t$ and $\tilde{x}_1 = k_l x_1$, where the characteristic quantities ω_l and k_l have

been defined in section 3. We can then introduce the non-dimensional form of the considered displacements as

$$\tilde{u}_i^l := \frac{u_i^l}{\alpha_i^l} = e^{j(\tilde{\omega}\tilde{t}-\tilde{k}_l^p\tilde{x}_1)}, \tag{24}$$

$$\tilde{u}_r^l := \frac{u_r^l}{\alpha_i^l} = \tilde{\alpha}_r^l e^{j(\tilde{\omega}\tilde{t}+\tilde{k}_l^p\tilde{x}_1)} + \tilde{\beta}_r^l e^{j(\tilde{\omega}t-j\tilde{k}_l^s\tilde{x}_1)}, \tag{25}$$

$$\tilde{u}_t^l := \frac{u_t^l}{\alpha_i^l} = \tilde{\alpha}_t^l e^{j(\tilde{\omega}\tilde{t}-\tilde{k}_l^p\tilde{x}_1)} + \tilde{\beta}_t^l e^{j(\tilde{\omega}t+j\tilde{k}_l^s\tilde{x}_1)}, \tag{26}$$

where clearly we set $\tilde{\alpha}_r^l = \alpha_r^l/\alpha_i^l$, $\tilde{\beta}_r^l = \beta_r^l/\alpha_i^l$, $\tilde{\alpha}_t^l = \alpha_t^l/\alpha_i^l$ and $\tilde{\beta}_t^l = \beta_t^l/\alpha_i^l$, where $\tilde{k}_l^p$ and $\tilde{k}_l^s$ are given by Eqs. (14) and where the dimensionless frequency $\tilde{\omega} = \omega/\omega_l$ has been defined in section 3.

It is clear that once the frequency and the first and second gradient elasticity parameters are given, the only unknowns of the reflection/transmission problem are the four amplitudes $\tilde{\alpha}_r^l$, $\tilde{\beta}_r^l$, $\tilde{\alpha}_t^l$ and $\tilde{\beta}_t^l$. These four scalar unknowns can be found for each of the three types of constraints introduced by considering Eqs. $(18)_1$, $(21)_1$ and $(23)_1$ respectively which only involve the longitudinal displacement. In conclusion, if we notice that here the first component of $[|\mathbf{u}|]$ takes the form $[|u_1|] = u_i^l - u_r^l - u_t^l$, and if we replace the wave form of the longitudinal displacement field in the non-dimensional version of equations $(18)_1$, $(21)_1$ and $(23)_1$ at $x_1 = 0$, we can finally recover the expression of the four amplitudes for each of the three types of constraints considered.

- *Generalized internal clamp*.

  As for the generalized internal clamp, the non-dimensional jump conditions (18) in the considered case in which the two continua on the two sides of S have the same material properties simply read

  $$[|\tilde{u}_1|] = 0, \quad [|\tilde{u}_1'|] = 0, \quad \left[\left|\tilde{u}_1' - \epsilon_l^2\tilde{u}_1'''\right|\right] = 0, \quad [|\tilde{u}_1''|] = 0, \tag{27}$$

  where, with a slight abuse of notation, we indicate with an apex the derivation operation with respect to the dimensionless space variable $\tilde{x}_1$. Replacing the aforementioned wave form for non-dimensional displacements in these boundary conditions we calculate the following non-dimensional amplitudes for longitudinal waves

  $$\tilde{\alpha}_r^l = 0, \quad \tilde{\beta}_r^l = 0, \quad \tilde{\alpha}_t^l = 1, \quad \tilde{\beta}_t^l = 0. \tag{28}$$

  This means that in the case of a perfect internal clamp at the surface S, the incident wave is completely transmitted. This result is not astonishing if we think that the two materials on both sides of S have been chosen to have the same material properties: indeed, it is as if there were no discontinuity at all and hence the incident wave proceeds unperturbed across the surface S.

- *Generalized elastic internal hinge*.

  As for the generalized elastic internal hinge between two continua with the same material properties, the non-dimensional form in the normal direction of jump conditions (21) reads

  $$\tilde{k}_S^n\,[|\tilde{u}_1|] = \left(\tilde{u}_1' - \epsilon_l^2 u_1'''\right)^+, \quad \left[\left|\tilde{u}_1' - \epsilon_l^2 u_1'''\right|\right] = 0, \quad (\tilde{u}_1'')^+ = 0, \quad (\tilde{u}_1'')^- = 0, \tag{29}$$

  where we introduced the dimensionless rigidity $\tilde{k}_S^n = k_S^n/(k_l(\lambda+2\mu))$. This non-dimensional choice implies that when $\tilde{k}_S^n = 1$ then the dimensional rigidity takes the value $k_S^n = k_l(\lambda+2\mu)$. The physical meaning of the rigidity $\tilde{k}_S^n$ can be intuitively got by thinking to the considered constraint as a series of elastic springs (of rigidity $\tilde{k}_S^n$) joining the two sides of the discontinuity. When $\tilde{k}_S^n$ goes to infinity, then the springs become infinitely stiff so that the displacement on the two sides of the discontinuity takes the same value and the introduced constraint particularizes to a generalized internal hinge. We explicitly remark that the non-dimensional form of the rigidity previously introduced is just one possible choice: this choice does not affect the physical interpretation of the limiting value of $\tilde{k}_S^n$ which we have just given.

  It is easy to prove that in the limit case of the elastic constant $\tilde{k}_S^n$ to infinity these boundary conditions reduce to

  $$[|\tilde{u}_1|] = 0, \quad \left[\left|\tilde{u}_1' - \epsilon_l^2 u_1'''\right|\right] = 0, \quad (\tilde{u}_1'')^+ = 0, \quad (\tilde{u}_1'')^- = 0. \tag{30}$$

We will refer to this limit case as *generalized internal hinge* in virtue of the continuity of displacement which is imposed at the discontinuity surface. This constraint differs from the *generalized internal clamp* defined by means of Eqs. (27) because the double force (second derivative of displacement) is zero on both sides of the discontinuity, while it can take an arbitrary value in the case of the clamp (even if this value must be the same on both sides). The similarities of the considered 3D constraints with the classical internal hinge and clamp for Euler-Bernoulli beams can be immediately pointed out. Indeed, as far the generalized internal hinge is considered, equation $(30)_1$ (continuity of displacement) implies by duality the continuity of force (Eq. $(30)_2$), while the double forces (which parallels couples in classical beam theory) are arbitrary on both sides (Eqs. $(30)_3$ and $(30)_4$). As for the generalized internal clamp, it is easy to recognize that Eqs. $(27)_1$ and $(27)_3$ parallel the continuity of displacement and force respectively, Eq. $(27)_4$ gives continuity of double forces (continuity of couples in the case of Euler-Bernoulli beams) which also implies Eq. $((27)_2)$ by duality. Indeed this constraint is the 3D counterpart of the internal clamp used in the theory of beams.

Using the considered wave form for displacements in boundary conditions 29, the calculated non-dimensional amplitudes take the form

$$\tilde{\alpha}_r^l = \frac{\tilde{k}_l^p(\tilde{k}_l^p - j\tilde{k}_l^s)\{\tilde{k}_l^s\left[\tilde{k}_l^s\epsilon_l^2\left(\tilde{k}_l^s(\epsilon_l\tilde{k}_l^p)^2 + 2\tilde{k}_S^n\right) + 1\right] - 2\tilde{k}_S^n\}}{(\tilde{k}_l^p + j\tilde{k}_l^s)(\tilde{k}_l^p\tilde{k}_l^s\epsilon_l^2 - j)\left[(\tilde{k}_l^p\epsilon_l\tilde{k}_l^s)^2 + 2\tilde{k}_S^n\tilde{k}_l^s - j\tilde{k}_l^p(\tilde{k}_l^s - 2\tilde{k}_S^n)\right]}$$

$$\tilde{\beta}_r^l = \frac{2(\tilde{k}_l^p)^2\left(\epsilon_l^2(\tilde{k}_l^p)^2 + 1\right)\left[(\tilde{k}_l^p\epsilon_l\tilde{k}_l^s)^2 + \tilde{k}_S^n\tilde{k}_l^s - j\tilde{k}_l^p(\tilde{k}_l^s - \tilde{k}_S^n)\right]}{(\tilde{k}_l^p + j\tilde{k}_l^s)\tilde{k}_l^s(\tilde{k}_l^p\tilde{k}_l^s\epsilon_l^2 - j)\left[(\tilde{k}_l^p\epsilon_l\tilde{k}_l^s)^2 + 2\tilde{k}_S^n\tilde{k}_l^s - j\tilde{k}_l^p(\tilde{k}_l^s - 2\tilde{k}_S^n)\right]}$$

$$\tilde{\alpha}_t^l = \frac{2\tilde{k}_l^s(\tilde{k}_l^s + j\tilde{k}_l^p)\tilde{k}_S^n\left[(\epsilon_l\tilde{k}_l^p)^2 + 1\right]}{(\tilde{k}_l^p + j\tilde{k}_l^s)(\tilde{k}_l^p\tilde{k}_l^s\epsilon_l^2 - j)\left[(\tilde{k}_l^p\epsilon_l^2\tilde{k}_l^s)^2 + 2\tilde{k}_S^n\tilde{k}_l^s - j\tilde{k}_l^p(\tilde{k}_l^s - 2\tilde{k}_S^n)\right]}$$

$$\tilde{\beta}_t^l = \frac{2(\tilde{k}_l^p)^2(\tilde{k}_l^s + j\tilde{k}_l^p)\tilde{k}_S^n\left((\epsilon_l\tilde{k}_l^p)^2 + 1\right)}{(\tilde{k}_l^p + j\tilde{k}_l^s)\tilde{k}_l^s(\tilde{k}_l^p\tilde{k}_l^s\epsilon_l^2 - j)\left[(\tilde{k}_l^p\epsilon_l\tilde{k}_l^s)^2 + 2\tilde{k}_S^n\tilde{k}_l^s - j\tilde{k}_l^p(\tilde{k}_l^s - 2\tilde{k}_S^n)\right]}$$

In the limit of elastic constant $\tilde{k}_S^n$ to infinity we have the case of the internal hinge and the calculated non-dimensional amplitudes take the following simplified form

$$\begin{aligned}
\tilde{\alpha}_r^l &= \frac{j\tilde{k}_l^p[1 - \epsilon_l^2(\tilde{k}_l^s)^2]}{(\tilde{k}_l^p + j\tilde{k}_l^s)(-j + \epsilon_l^2\tilde{k}_l^p\tilde{k}_l^s)}, \quad \tilde{\beta}_r^l = \frac{(\tilde{k}_l^p)^2[1 + \epsilon_l^2(\tilde{k}_l^p)^2]}{\tilde{k}_l^s(\tilde{k}_l^p + j\tilde{k}_l^s)(-j + \epsilon_l^2\tilde{k}_l^p\tilde{k}_l^s)}, \\
\tilde{\alpha}_t^l &= \frac{\tilde{k}_l^s[1 + \epsilon_l^2(\tilde{k}_l^p)^2]}{(\tilde{k}_l^p + j\tilde{k}_l^s)(-j + \epsilon_l^2\tilde{k}_l^p\tilde{k}_l^s)}, \quad \tilde{\beta}_t^l = \frac{(\tilde{k}_l^p)^2[1 + \epsilon_l^2(\tilde{k}_l^p)^2]}{\tilde{k}_l^s(\tilde{k}_l^p + j\tilde{k}_l^s)(-j + \epsilon_l^2\tilde{k}_l^p\tilde{k}_l^s)}.
\end{aligned} \tag{31}$$

- *Generalized 3D internal roller*.

Finally, if we consider a generalized roller between two continua with the same material properties, the non-dimensional form of jump conditions (23) reads

$$[|\tilde{u}_1'|] = 0, \quad (\tilde{u}_1' - \epsilon_l^2 u_1''')^+ = 0, \quad (\tilde{u}_1' - \epsilon_l^2 u_1''')^- = 0, \quad [|\tilde{u}_1''|] = 0,$$

Using the considered wave form for dimensionless displacements in these boundary conditions we get the following values for non-dimensional amplitudes

$$\begin{aligned}
\tilde{\alpha}_r^l &= \frac{k_l^s[1 + \epsilon_l^2(\tilde{k}_l^p)^2]}{(\tilde{k}_l^p + j\tilde{k}_l^s)(-j + \epsilon_l^2\tilde{k}_l^p\tilde{k}_l^s)}, \quad \tilde{\beta}_r^l = \frac{(\tilde{k}_l^p)^2[1 + \epsilon_l^2(\tilde{k}_l^p)^2]}{\tilde{k}_l^s(\tilde{k}_l^p + j\tilde{k}_l^s)(-j + \epsilon_l^2\tilde{k}_l^p\tilde{k}_l^s)}, \\
\tilde{\alpha}_t^l &= \frac{j\tilde{k}_l^p[-1 + \epsilon_l^2(\tilde{k}_l^s)^2]}{(\tilde{k}_l^p + j\tilde{k}_l^s)(-j + \epsilon_l^2\tilde{k}_l^p\tilde{k}_l^s)}, \quad \tilde{\beta}_t^l = \frac{-(\tilde{k}_l^p)^2[1 + \epsilon_l^2(\tilde{k}_l^p)^2]}{\tilde{k}_l^s(\tilde{k}_l^p + j\tilde{k}_l^s)(-j + \epsilon_l^2\tilde{k}_l^p\tilde{k}_l^s)}.
\end{aligned} \tag{32}$$

Let us now consider the case of transverse waves travelling in the x_1 direction. As done for longitudinal waves, we introduce the incident transversal displacement as:

$$u_i^t = \alpha_i^t e^{j(\omega t - k_2^p x_1)},$$

where α_i^t is the amplitude of the incident transverse wave which we assume to be known and k_2^p is the wave number associated to a transverse wave propagating in the x_1 direction. We then call u_r^t and u_t^t the reflected and transmitted transverse wave respectively. According to the geometry of the considered problem the reflected and transmitted waves take the following form

$$u_r^t = u_r^{tp} + u_r^{ts} = \alpha_r^t e^{j(\omega t + k_2^p x_1)} + \beta_r^t e^{j(\omega t + j k_2^s x_1)},$$

where α_r^t is the amplitude of the propagative reflected wave travelling in the $-x_1$ direction and β_r^t is the amplitude of the standing reflected wave. Note that the standing reflected wave goes to zero as x_1 approaches $-\infty$. Moreover, the transmitted wave is defined as

$$u_t^t = u_t^{tp} + u_t^{ts} = \alpha_t^t e^{j(\omega t - k_2^p x_1)} + \beta_t^t e^{j(\omega t - j k_2^s x_1)},$$

The obtained equations for transversal waves are formally analogous to longitudinal ones, since one has just to replace $\tilde{u}_1$ with $\tilde{u}_2$ and all the subscripts and superscripts l with the subscripts and superscripts t respectively. Repeating the calculations performed for longitudinal waves, we can then calculate the four amplitudes $\tilde{\alpha}_r^t$, $\tilde{\beta}_r^t$, $\tilde{\alpha}_t^t$ and $\tilde{\beta}_t^t$ of the reflected and transmitted transverse waves for the three considered types of constraints imposed at the surface S.

6 Dependence of transmission and reflection coefficients on second gradient elastic moduli

In this section we will show plots displaying the reflection and transmission coefficients at discontinuity surfaces of the three types considered before as functions of second gradient elastic moduli. To do so, we start by noticing that owing to the fact that the problem is completely uncoupled in the longitudinal and transversal displacements, we can account separately for the energy fluxes of longitudinal and transversal waves. Moreover, due to the linearity of the problem in study, we can consider separate contributions for the fluxes of the incident, reflected and transmitted waves which, starting from expression (10), can be written in terms of the introduced non-dimensional variables respectively as

$$\begin{aligned}
\tilde{H}_i^l(\tilde{x}_1,\tilde{t}) &= (\alpha_i^l)^2 k_l \omega_l (\lambda+2\mu)\left[-\left(\tilde{u}_i^l\right)'\dot{\tilde{u}}_i^l + \epsilon_l^2\left(\left(\tilde{u}_i^l\right)'''\dot{\tilde{u}}_i^l - \left(\tilde{u}_i^l\right)''\left(\dot{\tilde{u}}_i^l\right)'\right)\right],\\
\tilde{H}_r^l(\tilde{x}_1,\tilde{t}) &= (\alpha_i^l)^2 k_l \omega_l (\lambda+2\mu)\left[-\left(\tilde{u}_r^l\right)'\dot{\tilde{u}}_r^l + \epsilon_l^2\left(\left(\tilde{u}_r^l\right)'''\dot{\tilde{u}}_r^l - \left(\tilde{u}_r^l\right)''\left(\dot{\tilde{u}}_r^l\right)'\right)\right],\\
\tilde{H}_t^l(\tilde{x}_1,\tilde{t}) &= (\alpha_i^l)^2 k_l \omega_l (\lambda+2\mu)\left[-\left(\tilde{u}_t^l\right)'\dot{\tilde{u}}_t^l + \epsilon_l^2\left(\left(\tilde{u}_t^l\right)'''\dot{\tilde{u}}_t^l - \left(\tilde{u}_t^l\right)''\left(\dot{\tilde{u}}_t^l\right)'\right)\right],
\end{aligned} \tag{33}$$

where we recall that, with a slight abuse of notation, the apex and the dot stand here for the derivation operations with respect to the introduced dimensionless space and time variables. A simple inspection of Eqs. (33), and recalling that the displacement field take the wave form (11), shows that for higher frequencies and shorter wavelengths (i.e. larger wave number k) the amount of energy transported because of second gradient effects increases. The corresponding energy fluxes for transversal waves are formally analogous and are obtained from the previous ones just replacing everywhere the apex l with the apex t and the parameter ϵ_l with the parameter ϵ_t. In order to be able to calculate the reflection and transmission coefficients for the considered problem, we substitute in Eqs. (33) the wave forms (24) , (25) and (26) for the displacements and we calculate the integrals over the period $2\pi/\tilde{\omega}$ of the introduced energy fluxes. It can be shown that, due to conservation of energy, these integrals do not depend on the space variable $\tilde{x}_1$. Owing to this independence on the variable $\tilde{x}_1$, in order to simplify calculations, we can simply introduce these integrals as

$$J_i^l = \int_0^T \tilde{H}_i^l(0,\tilde{t})d\tilde{t}, \qquad J_r^l = \int_0^T \tilde{H}_i^l(-\infty,\tilde{t})d\tilde{t}, \qquad J_t^l = \int_0^T \tilde{H}_i^l(+\infty,\tilde{t})d\tilde{t}.$$

We are then finally able to introduce the reflection and transmission coefficients for longitudinal waves as

$$R_l := \frac{J_r^l}{J_i^l}, \qquad T_l := \frac{J_t^l}{J_i^l},$$

which are such that $R_l + T_l = 1$. The reflection and transmission coefficients R_t and T_t for transversal waves are formally analogous.

We show in the following figures the behaviour of reflection and transmission coefficients in terms of both the second gradient parameter ϵ and the frequency ω. These figures refer to both the longitudinal and transversal case: one has just to interpret ϵ as ϵ_l and ϵ_t respectively.

Referring to Fig.3, we can start noticing that, when the second gradient parameter tends to zero, the generalized internal hinge (continuity of displacement and arbitrary normal derivative of displacement at the considered surface of discontinuity)

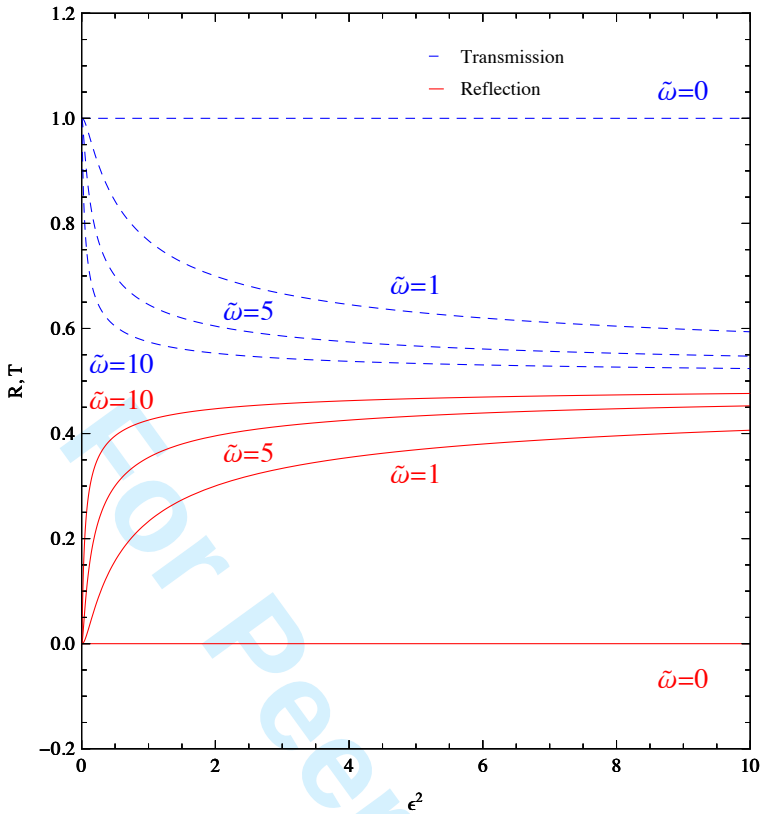

Fig. 3 Reflection and transmission coefficients for a generalized internal hinge ($k_S^n \to \infty$) as a function of the second gradient parameter ϵ^2 and for different values of the non-dimensional frequency. The plots for the generalized internal roller are completely specular: the blue dashed lines must be referred to the reflection coefficient, while the red lines must be referred to the transmission coefficient.

implies that all the energy is transmitted independently on the value of the frequency. If the second gradient parameter is not vanishing, then the value of the frequency starts to play a role on the amount of energy which is transmitted or reflected. In particular, for very low frequencies (approaching to zero), the energy of the travelling wave continue to be almost completely transmitted independently on the value of the second gradient parameter ϵ^2. When increasing the frequency, the fact that the normal derivative of displacement at the discontinuity can take arbitrary value on both sides starts to play a role in the sense that the amount of reflected energy starts to increase, while the amount of transmitted energy decreases. This behavior can be directly related with the fact that, as it is well known (see e.g. [70], [71], [96] and [97]), second gradient theories take into account the existence of an underlying micro-structure even if remaining in the framework of a macroscopic model. More particularly, the fact that, for a given value of the second gradient parameter, an increasing frequency implies an increased amount of reflected energy can be explained if one thinks that the wavelength of the travelling wave decreases and becomes comparable to the characteristic length of the heterogeneities that are present in the material at a microscopic level. In other words, for very large wavelengths (small frequencies) the medium can be reasonably considered homogeneous even very close to the interface of discontinuity. In this case, when the considered wave reaches the interface, the continuity of displacements guarantees that the wave can continue undisturbed its path across the discontinuity itself. On the other hand, for smaller wavelengths (higher frequencies) the medium cannot longer be considered homogeneous since the wave starts interacting with the underlying microscopic heterogeneities. More precisely, high frequency waves activate “long range interactions” at the microscopic level which result in an increasing amount of energy transported in the bulk because of the time derivative of displacement gradient (see Eqs. (33) and subsequent considerations or, more generally, Eq. (4)). However, normal strains (normal gradient of displacement) at the two sides of the discontinuity interface are uncoupled because of the chosen boundary condition (generalized internal hinge) so that this amount of energy propagating because of microscopic interactions is actually reflected at the interface. The two just considered circumstances can be physically interpreted as follows: high frequency waves propagating in the bulk activate long-range interactions at a microscopic level and induce coupled deformations of close microscopic deformable structures, with a non-negligible amount of energy travelling because of this coupling. However, since at the considered interface we

assume that close microscopic structures situated at different sides are uncoupled, the amount of energy transported by these microscopically-interacting structures can only be reflected. Always referring to Fig.3, we can finally remark that, for a fixed value of the frequency (and hence of the wavelength $1/k_l$), the amount of reflected energy increases for increasing values of the second gradient parameter up to the value $\epsilon^2 \approx 4$ and then it takes an almost constant value for greater values of ϵ^2. This is completely sensible and it means that, for a fixed value of the wavelength $(1/k_l)$, the amount of reflected energy increases with the value of the second gradient parameter ($\epsilon = L_l\, k_l$) in the range of values in which ϵ is sufficiently close to one (or equivalently in the range in which the considered wavelength is comparable to the second gradient characteristic length L_l). In this range, the amount of reflected energy becomes more and more important when ϵ increases since the considered wavelength becomes comparable to the value of the second gradient characteristic length. For values of the second gradient parameter larger than four (or equivalently $L_l > 4/k_l$) the amount of reflected (transmitted) energy has a less relevant variation.

Considerations for the generalized internal roller are completely reversed with respect to those just made for the generalized internal hinge and can be deduced from Fig.3 reversing the curves of reflection and transmission coefficients. We start by noticing that when the second gradient parameter tends to zero, all the energy is reflected at the considered interface. Moreover, we notice that for very small values of the frequency (approaching to zero) approximately the total amount of the energy is still reflected independently on the value of the second gradient parameter. As before, this can be explained with the fact that, as the wavelength is sufficiently large then the medium can be considered homogeneous, and that the considered constraint allows arbitrary displacements on both sides of the considered interface. In some sense, it is like the interface was a free interface (no other medium on the other side) so that the incident wave can be reflected only. On the other hand, for non-vanishing values of the second gradient parameter and for increasing values of the frequency, some of the incident energy starts to be transmitted. As before, this can be explained with the fact that, for decreasing wavelengths, the wave starts interacting with the micro-structure on the other side of the discontinuity surface. This means that the heterogeneities "start moving" at the microscopic level and create some mechanical interactions between the two sides of the considered interface, so allowing some energy transmission. The fact that for a fixed frequency the generalized roller allows for an increasing transmitted energy when increasing the value of the second gradient parameter up to the value $\epsilon^2 \approx 4$ can be as before be explained by considering that the second gradient interactions becomes more important when the wavelength becomes comparable to the characteristic second gradient length.

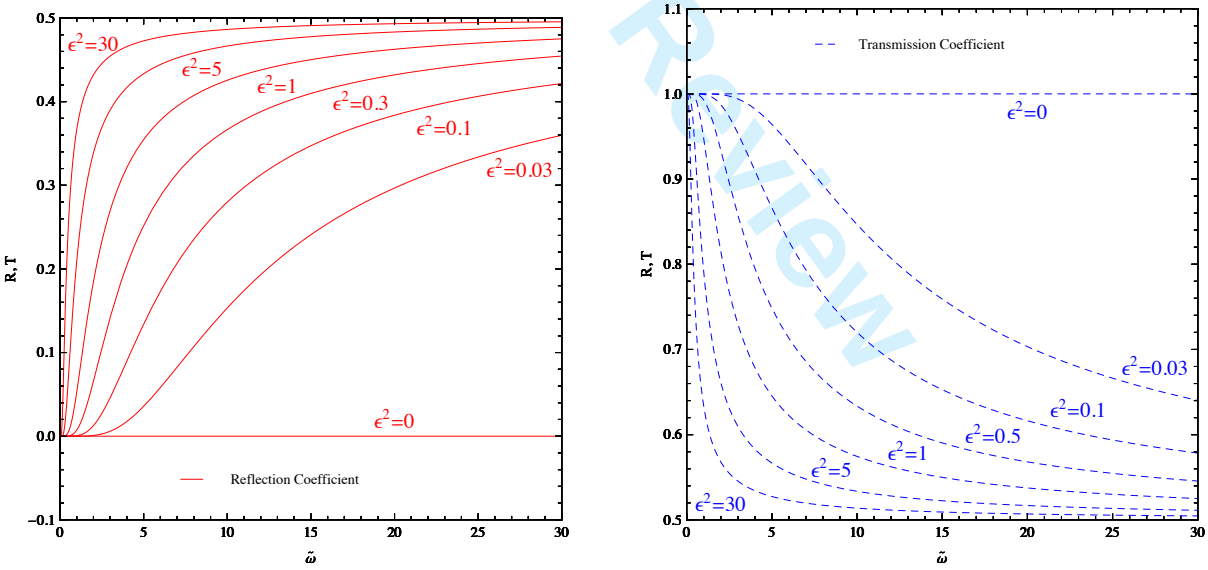

Fig. 4 Reflection and transmission coefficients for a generalized internal hinge ($k_S^n \to \infty$) as a function of the non-dimensional frequency and for different values of the second gradient parameter ϵ^2. The plots for the generalized internal roller are completely specular: the blue dashed lines must be referred to the reflection coefficient, while the red lines must be referred to the transmission coefficient.

Referring to Fig.4, we can notice once again that, for a generalized internal hinge and once fixed the value of the second gradient parameter, an increase in the frequency results in an increased amount of reflected energy and hence in a decreasing of the transmitted one. Moreover, one also recovers that, for sufficiently large frequencies $\tilde{\omega}$, the amount of reflected energy increases with $\tilde{\omega}$ for values of the second gradient parameter up to a given threshold, while it keeps an almost constant value for values of the second gradient parameter larger than the threshold: this behavior was already noticed when analysing

Fig.3. Indeed, in Fig.4 we can indirectly observe a boundary layer effect which was not detectable in the previous figure: a very small increase in the frequency imply a sudden increase of the amount of reflected energy for big values of the second gradient parameter. This means that for high values of the second gradient parameter the characteristic length which measures the spacing between the heterogeneities at the microscopic level is so large (i.e. the heterogeneities are so dispersed) that the energy can be completely reflected only when the wavelength tends to infinity (frequency tends to zero). In other words, the heterogeneities are dispersed enough that the medium can be considered as homogeneous only for very large wavelengths and, for some reason (e.g. very different stiffness of the inclusions with respect to the matrix), the presence of these heterogeneities cannot be neglected at the macroscopic level. Analogous considerations for the generalized internal roller can be done starting from Fig.4 and reversing the reflection and transmission coefficient.

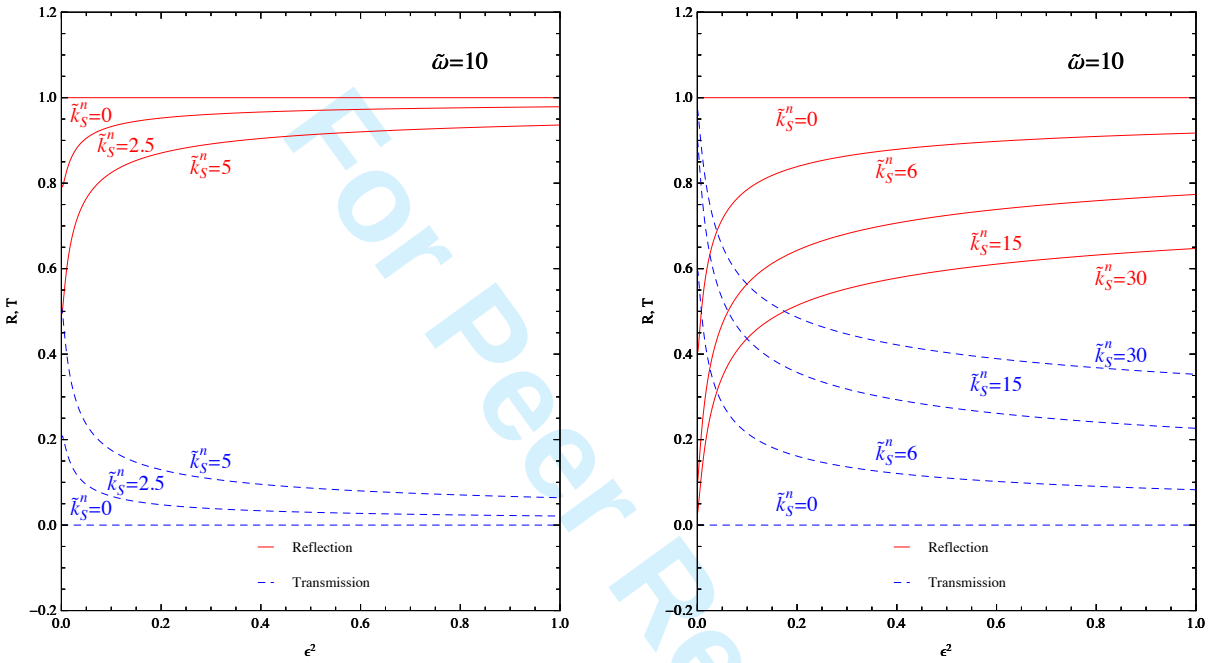

Fig. 5 Reflection and transmission coefficients for a generalized elastic internal hinge as a function of the second gradient parameter ϵ^2, for different values of the surface rigidity $k_S^n \in [0, 30]$ and for a fixed value of the non-dimensional frequency $\tilde{\omega} = 10$

Figure 5 shows reflection and transmission coefficients for a generalized elastic internal hinge as a function of the second gradient parameter, for a fixed value of the frequency and for different values of the elastic rigidity at the interface. As we already noticed this constraint reduce to the generalized internal hinge when the rigidity $\tilde{k}_S^n$ tends to infinity. It can be remarked from this figure that when the elastic rigidity tends to zero, then this constraint reduces to the generalized internal roller. We can notice that a critical value of the elastic rigidity $\tilde{k}_S^n = 5$ exists corresponding to which a switch can be observed. More precisely, for values of the rigidity between 0 and 5 the larger amount of energy is reflected so that the considered constraint basically behave like a generalized internal roller. For values of the rigidity bigger than 5 a critical value of the second gradient parameter exists such that for ϵ^2 smaller than this critical value the bigger amount of energy is transmitted (the constraint behave as a generalized internal roller), while for for ϵ^2 bigger than this critical value the larger amount of energy is reflected (the constraint behave as a generalized internal hinge).

As for Fig.6, considerations analogous to those previously done before can be repeated. We start remarking that in the case of a generalised elastic internal hinge a critical value of the frequency (between $\tilde{\omega} = 1$ and $\tilde{\omega} = 2$) exists corresponding to which another switch can be observed. More precisely, for values of the frequency smaller than this critical value the larger amount of energy is transmitted and the considered constraint basically behave like a generalized internal hinge. For values of the frequency bigger than this critical value, a critical value of the second gradient parameter exists such that for ϵ^2 smaller than this critical value the larger amount of energy is transmitted (the constraint behaves more like a generalized internal hinge), while for higher values of the second gradient parameter the larger amount of energy is reflected (the constraint behaves more like a generalized internal roller). This behavior can be explained if one thinks that the considered constraint can be thought as a surface distribution of elastic springs of rigidity $\tilde{k}_S^n$ between the two sides of the considered interface. For a fixed value of $\tilde{k}_S^n$ and for very small frequencies it is reasonable that the spring remains at rest so that the jump of displacement between a point on one side of the discontinuity and the corresponding point on the other side is

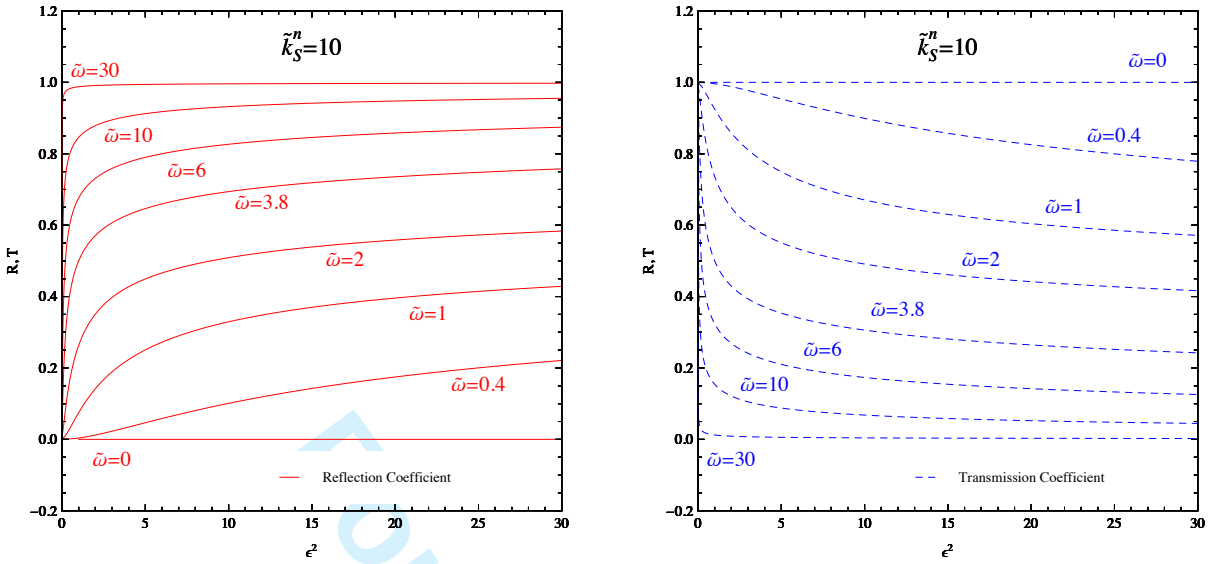

Fig. 6 Reflection and transmission coefficients for a generalized elastic internal hinge as a function of the second gradient parameter ϵ^2, for $\tilde{k}_S^n = 10$ and for different values of $\tilde{\omega} \in [0, 30]$.

vanishing and the energy can be transmitted through the discontinuity (the constraint behaves like a generalized internal hinge). When increasing the frequency, it is easy to understand that a threshold value (of the frequency) exists corresponding to which the springs start elongating and hence a loss of contact between the two sides of the interface arrives resulting in a decreasing of the transmitted energy. How the energy can be trapped in motions of extra degrees of freedom localized at the interface could be studied using the methods presented in [14] and [13]. The critical value of the second gradient parameter can be explained by thinking that for ϵ^2 smaller than this critical value the heterogeneities at the microscopic level can be considered concentrated enough that they are able to create a sufficient quantity of long range interactions between the two sides of the discontinuity surface so that a larger amount of energy continue to be transmitted. For values of ϵ^2 larger than the critical value the underlying heterogeneities are so dispersed that the long range interactions between the two sides of the discontinuity drastically reduce so resulting in a decrease of the transmitted energy. Clearly if the value of the frequency becomes very large then the springs can elongate of a big amount and the two sides of the discontinuity become so far away that the micro-heterogeneities are not able to create any long range interaction any more and the energy is completely reflected (generalized internal roller) independently on the characteristic second gradient parameter.

7 Conclusions

The presented results show that it is conceivable to design an experimental method for getting estimates of some second gradient elastic moduli. Indeed, we propose to use a discontinuity surface between two macroscopically homogeneous second gradient solids to perform measurements of reflection and transmission coefficients at this interface: the presented results seem to supply a method for measuring the bulk properties of considered continua starting from these coefficients. The results obtained in the last section of this paper show that the concepts presented here may be of interest as the boundary layer which may arise greatly influences wave transmission and reflection even in the considered simple cases. We assume that the discontinuity surface is the only possible localization of displacement (and normal gradient of displacement) eventual jumps. Moreover we also consider interfaces on which surface elastic energy is concentrated. More complicated discontinuity surfaces may be conceived carrying mechanical properties which may directly influence transmission and reflection coefficients. Even if the investigation of the behavior of such more general discontinuity surfaces is of importance, the simplest discontinuity we considered here seems suitable for the conception of an effective experimentation.

The field of second gradient continuum theories, even if it is attracting much more interest in the last years, still receives some criticism due to the fact that no experimental measurement techniques of second gradient elastic moduli are available in the literature. Performing the proposed experimental indirect measurements by using reflection and transmission of plane waves would undoubtedly be of great scientific and technological interest. Measuring these moduli for a certain class of solids would then be useful as a starting point for further investigations. More complicated subsequent analyses should

involve the study of structured interfaces between second gradient solids, or permeable and impermeable interfaces between different porous media in presence of Darcy-type fluid flow, or interfaces between damaged and undamaged solids.

Finally, we want to state that a very strong indication of the potential utility of the proposed analysis is given by the experimental evidence obtained by [62]. The experimentally measured dependence of the reflected and transmitted signals at the "prepared" surface between dentine and surrounding fluid greatly resembles the dependence which we have obtained theoretically for the here treated case of generalized internal roller . The theoretical previsions which we obtain seems closer to experimental evidence than the previsions obtained, starting from a different einsatz, by [62] themselves. Indeed, they assume that: i) the interface is constituted by a Cauchy continuum with space-varying elastic moduli, ii) the dentine can be modelled as a Cauchy continuum. We expect that the development of a model of porous second gradient material saturated by a fluid in contact with a pure fluid through a suitably structured interface should provide a deeper theoretical understanding of aforementioned experimental evidence.

References

[1] R. Abeyaratne, N. Triantafyllidis, An investigation of localization in a porous elastic material using homogenization theory. *Trans. ASME J. Appl. Mech.* **51**(3), 481-486 (1984).

[2] R. K. Abu Al-Rub, Modeling the interfacial effect on the yield strength and flow stress of thin metal films on substrates. *Mechanics Research Communications* **35** 65-72 (2008).

[3] E. C. Aifantis, Gradient Deformation Models at Nano, Micro, and Macro Scales. Journal of Engineering Materials and Technology, 121(2), 189–202 (1999)

[4] E. C. Aifantis, Update on a class of second gradient theories. *Mech. Materials* **35**, 259-280 (2003).

[5] J.-J. Alibert,P. Seppecher, F. Dell'Isola, Truss modular beams with deformation energy depending on higher displacement gradients. *Math. Mech. Solids* **8**(1), 51-73 (2003).

[6] C. Banfi, A. Marzocchi and A. Musesti, On the principle of virtual powers in continuum mechanics. *Ricerche di Matematica* 55, 299-310 (2006).

[7] S.Bardenhagen, N. Triantafyllidis, Derivation of higher order gradient continuum theories in 2,3-D nonlinear elasticity from periodic lattice models. *J. Mech. Phys. Solids* **42**(1), 111-139 (1994).

[8] V. Berdichevsky, Variational Principles of Continuum Mechanics, Springer, (2009).

[9] J.L. Bleustein, A note on the boundary conditions of Toupin's strain-gradient theory. *International Journal of Solids and Structures*, **3**(6), 1053-1057 (1967).

[10] A. Carcaterra, E. Ciappi, Prediction of the compressible stage slamming force on rigid and elastic systems impacting on the water surface. *Nonlinear Dynamics* **21**(2), 193-220 (2000).

[11] A. Carcaterra, E. Ciappi, A. Iafrati, *et al*. Shock spectral analysis of elastic systems impacting on the water surface. *JOURNAL OF SOUND AND VIBRATION* **229**(3), 579-605 (2000).

[12] A. Carcaterra, Ensemble energy average and energy flow relationships for nonstationary vibrating systems. *Journal of the Acoustical Society of America* **288**(3), 751-790 (2005).

[13] A. Carcaterra, A. Akay, I.M. Koc, Near-irreversibility in a conservative linear structure with singularity points in its modal density. *Journal of the Acoustical Society of America* **119**(4), 2141-2149 (2006).

[14] A. Carcaterra, A. Akay, Theoretical foundations of apparent-damping phenomena and nearly irreversible energy exchange in linear conservative systems. *Journal of the Acoustical Society of America* **121**(4) 1971-1982 (2007).

[15] M.O.M. Carvalho & M. Zindeluk, Active control of waves in a Timoshenko beam. *Int. J. Solids Struct.* **38**, 1749-1764 (2001).

[16] P. Casal, La capillarité interne, *cahier du group francais de rhéologie, CNRS* **6**, 31-37, (1961).

[17] P. Casal, La théorie du second gradient et la capillarité. C. R. Acad. Sci. Paris, t. 274, Série A (1972) 1571–1574.

[18] P. Casal & H. Gouin, Relation entre l'équation de l'énergie et l'équation du mouvement en théorie de Korteweg de la capillarité. *C.R. Acad. Sci. Paris* **300** II 7, 231-235 (1985).

[19] F. Collin, R. Chambon, R. Charlier, A finite element method for poro mechanical modelling of geotechnical problems using local second gradient models. *Int. J. Num. Meth. Engng.* **65**, 1749-1772 (2006).

[20] E. Cosserat & F. Cosserat, Note sur la théorie de l'action euclidienne. Paris, Gauthier-Villars, (1908).

[21] E. Cosserat & F. Cosserat, Sur la théorie des corps déformables. Herman, Paris, (1909).

[22] A. Culla, A. Sestieri, A. Carcaterra, Energy flow uncertainties in vibrating systems: Definition of a statistical confidence factor. *Mechanical Systems and Signal Processing* **17** (3), 635-663 (2003).

[23] N. Daher, G. A. Maugin, Virtual power and thermodynamics for electromagnetic continua with interfaces. *J. Math. Phys.* **27**(12), 3022-3035 (1986a)

[24] N. Daher, G. A. Maugin, The method of virtual power in continuum mechanics. Application to media presenting singular surfaces and interfaces. *Acta Mech* **60**(3-4), 217-240 (1986b)

[25] P. G. de Gennes, Some effects of long range forces on interfacial phenomena. *J. Physique Lettres* **42**, L-377, L-379 (1981).

[26] F. dell'Isola & P. Seppecher, The relationship between edge contact forces, double force and interstitial working allowed by the principle of virtual power. *CRAS - Serie IIb: Mecanique, Physique, Chimie, Astronomie* **321**, 303-308 (1995).

[27] M. Degiovanni, A. Marzocchi, and A. Musesti, Cauchy fluxes associated with tensor fields having divergence measure. *Arch. Ration. Mech. Anal.* **147** 197-223 (1999).

[28] M. Degiovanni, A. Marzocchi and A. Musesti Edge-force densities and second-order powers. *Annali di Matematica 185*, 81-103 (2006).

[29] F. dellIsola, H. Gouin, P. Seppecher, Radius and Surface Tension of Microscopic Bubbles by Second Gradient Theory. *CRAS IIB Mechanics* **320**, 211-216 (1995).

[30] F. dellIsola, H. Gouin, G. Rotoli. Nucleation of Spherical Shell-Like Interfaces by Second Gradient Theory: Numerical Simulations. Eur. J. Mech., B/Fluids **15**(4), 545-568 (1996)

[31] F. dell'Isola & P. Seppecher, Edge Contact Forces and Quasi-Balanced Power. *Meccanica* **32** 33-52 (1997)

[32] F. dellIsola, A. Madeo, P. Seppecher, Boundary Conditions at Fluid-Permeable Interfaces in Porous Media: A Variational Approach. *Int. J. Solids Struct.* **46**, 3150-3164 (2009*a*).

[33] F. dell'Isola, G. Sciarra, S. Vidoli, Generalized Hooke's law for isotropic second gradient materials, *Proc. R. Soc. A* **465**, 2177-2196 (2009*b*).

[34] F. dell'Isola and P. Seppecher, Commentary about the paper " Hypertractions and hyperstresses convey the same mechanical information Continuum Mech. Thermodyn 22:163176 " by Prof. Podio Guidugli and Prof. Vianello and some related papers on higher gradient theories. Continuum Mechanics and Thermodynamics **22** 163-175 (2010).

[35] M. Destrade and G. Saccomandi, Waves in Nonlinear Pre-Stressed Materials, CISM Lecture Notes 495, Springer, (2007).

[36] J.E. Dunn, and J. Serrin, On the thermomechanics of interstitial working. *Arch. Rational Mech. Anal.* **88**(2), 95-133 (1985).

[37] V.I. Erofeyev, Wave Processes in Solids with Microstructure. World Scientific Publishing, Singapore (2003)

[38] G. E. Exadaktylos, I. Vardoulakis, Microstructure in linear elasticity and scale effects: a reconsideration of basic rock mechanics and rock fracture mechanics. *Tectonophysics* **335**(1-2), 81-109 (2001).

[39] A.C. Fannjiang, Y.-S. Chan, G.H. Paulino, Strain gradient elasticity for antiplane shear cracks: a hypersingular integrodifferential equation approach. *SIAM J. Appl. Math.* **62**(3), 1066-1091 (2001).

[40] S. Forest, Mechanics of generalized continua: construction by homogenization. *J.Phys.* IV France **8** (1998).

[41] S. Forest, M. Amestoy, S. Cantournet, G. Damamme, S. Kruch Mécanique des Milieux Continus ECOLE DES MINES DE PARIS Année 2005-2006

[42] S. L. Gavrilyuk, S. M. Shugrin, Media with state equations that depend on the derivatives. (Russian) Prikl. Mekh. Tekhn. Fiz. 37 (1996), no. 2, 35-49; translation in *J. Appl. Mech. Tech. Phys.* **37**(2), 177-189 (1996).

[43] S. Gavrilyuk, H. Gouin, Symmetric form of governing equations for capillary fluids. Trends in applications of mathematics to mechanics (Nice, 1998), 306-311, Chapman & Hall/CRC Monogr. Surv. Pure Appl. Math., 106, Chapman & Hall/CRC, Boca Raton, FL, 2000

[44] P. Germain, Sur l'application de la méthode des puissances virtuelles en mécanique des milieux continus. *C. R. Acad. Sci. Paris Série A-B* **274**, A1051-A1055 (1972).

[45] P. Germain, La méthode des puissances virtuelles en mécanique des milieux continus Premiere partie: Théorie du second gradient,*J. Mécanique* **12**(2), 235-274 (1973*a*).

[46] P. Germain, The method of virtual power in continuum mechanics Part 2: Microstructure, *S.I.A.M. J. Appl. Math.* **25:**(3), 556-575 (1973*b*).

[47] A.E. Green and R.S. Rivlin, Simple force and stress multipoles, *Arch. Rational Mech. Anal.*, **16**,325-353 (1964a)

[48] A.E. Green and R.S. Rivlin, Multipolar continuum mechanics, *Arch. Rational Mech. Anal.*, **17**, 113-147 (1964b).

[49] A.E. Green and R.S. Rivlin, Multipolar continuum mechanics: Functional theory. I, *Proc. Roy. Soc. Ser. A 284*, 303–324 (1965).

[50] J.- L. Guyader, Vibration in Continuous Media, ISTE Ltd, Chippenham (2006).

[51] J. G. Harris, Linear Elastic Waves, Cambridge University Press, Cambridge (2004).

[52] N. Kirchner and P. Steinmann, A unifying treatise on variational principles for gradient and micromorphic continua. *Philosophical Magazine* , **85**(33-35), 3875-3895 (2005).

[53] R. Larsson, S. Diebels, A second-order homogenization procedure for multi-scale analysis based on micropolar kinematics. *Internat. J. Numer. Methods Engrg.* **69**(12), 2485-2512 (2007).

[54] M. Lazar, G. A. Maugin, Defects in gradient micropolar elasticity—I: screw dislocation. Journal of the Mechanics and Physics of Solids 52, 2263 –2284 (2004a)

[55] M. Lazar, G. A. Maugin, Defects in gradient micropolar elasticity—II: edge dislocation and wedge disclination. Journal of the Mechanics and Physics of Solids 52, 2285 –2307 (2004b)

[56] M. Lazar, G. A. Maugin, Nonsingular stress and strain fields of dislocations and disclinations in first strain gradient elasticity. International Journal of Engineering Science 43 1157–1184 (2005)

[57] M. Lazar, G. A. Maugin and E. C. Aifantis, On dislocations in a special class of generalized elasticity. Phys. Stat. Sol. (b) 242(12), 2365–2390 (2005)

[58] M. Lazar, G. A. Maugin, A note on line forces in gradient elasticity. Mechanics Research Communications 33, 674–680 (2006)

[59] M. Lazar, G. A. Maugin, E. C. Aifantis, Dislocations in second strain gradient elasticity. International Journal of Solids and Structures 43, 1787–1817 (2006).

[60] M. Lucchesi, M. Silhavý, N. Zani, On the Balance Equation for Stresses Concentrated on Curves. *J. Elasticity* **90**, 209-223 (2008).

[61] A. Madeo, F. dellIsola, N. Ianiro and G. Sciarra, A Variational Deduction of Second Gradient Poroelasticity II: an Application to the Consolidation Problem. *J. Mech. Materials Struct.* **3**(4), 607625, (2008).

[62] O. Marangos, A. Misra, P. Spencer, and J.L. Katz, J.L., Scanning acoustic microscopy investigation of frequency-dependent reflectance of acid-etched human dentin using homotopic measurements, IEEE Transactions UFFC, (accepted) (2011).

[63] G. A. Maugin, A. C. Eringen, On the equations of the electrodynamics of deformable bodies of finite extent. *J. Mécanique* **16** (1), 101-147 (1977)
[64] G. A. Maugin, The method of virtual power in continuum mechanics: application to coupled fields. *Acta Mech*. **35**(1-2), 1-70 (1980)
[65] G. A. Maugin, A relativistic version of the principle of virtual power. Special issue dedicated to Prof. K. Kondo. *Internat. J. Engrg. Sci*. **19**(12), 1719-1730 (1981).
[66] G. A. Maugin and A. V. Metrikine, Mechanics of generalized continua. One hundred years after the Cosserats. Selected papers from the EUROMECH Colloquium 510 held in Paris, May 13–16, 2009. Edited by Gérard A. Maugin and Andrei V. Metrikine. *Advances in Mechanics and Mathematics*, **21**. Springer, New York, (2010).
[67] A.Marzocchi, and A. Musesti, Decomposition and integral representation of Cauchy interactions associated with measures. *Cont. Mech. Thermodyn*. **13**, 149-169 (2001).
[68] A. Marzocchi, A. Musesti, Balanced virtual powers in Continuum Mechanics. *Meccanica* **38**, 369-389 (2003).
[69] A. Menzel, P. Steinm'ann, On the Formulation of Higher Gradient Single and Polycrystal Plasticity. Le Journal de Physique IV 08 , Nr. Pr.8, 239-247 (1998).
[70] R.D. Mindlin, Second gradient of strain and surface tension in linear elasticity. *Int. J. Solids and Struct*. 1(4) ,417-438 (1965).
[71] R.D.Mindlin, H.F. Tiersten, Effects of couple-stresses in linear elasticity.*Arch. Rational Mech. Anal*. **11**, 415-448 (1962).
[72] R.D. Mindlin, N.N. Eshel, On first strain-gradient theories in linear elasticity. *International Journal of Solids and Structures* **4**(1), 109-124 (1968)
[73] A. Misra, Mechanistic Model for Contact between Rough Surfaces, *Journal of Engineering Mechanics*, ASCE, **123**(5), 475-484 (1997).
[74] A. Misra, Effect of asperity damage on friction behavior of single fracture. *Engineering Fracture Mechanics*, **69**(17), 1997-2014 (2002).
[75] A. Misra, and O. Marangos, Application of a Micromechanical Model to Wave Propagation through Nonlinear Rough Interfaces Under Stress. ULTRASONICS SYMPOSIUM, VOLS 1-5, PROCEEDINGS Book Series: ULTRASONICS SYMPOSIUM Pages: 309-312 (2006).
[76] A. Misra and O. Marangos, Parametric Studies of Wave Propagation Through Imperfect Interfaces Using Micromechanics Based Effective Stiffness. *Review of Progress in Quantitative Nondestructive Evaluation*, **27B**, 1074-1081 (2008*a*).
[77] A. Misra and O. Marangos, Micromechanical Model of Rough Contact between Rock Blocks with Application to Wave Propagation.*Acta Geophysica*, **56**(4), 1109-1128 (2008*b*).
[78] A. Misra and O. Marangos, Effect of Contact Viscosity and Roughness on Interface Stiffness and Wave Propagation.*Review of Progress in Quantitative Nondestructive Evaluation*, **28A**, 105-112 (2009).
[79] A. Misra and S. Huang, Micromechanics based stress-displacement relationships of rough contacts: Numerical implementation under combined normal and shear loading. *Computer Modeling in Engineering and Sciences*, **52**(2), 197-215 (2009).
[80] A. Misra and O. Marangos, Rock Joint Micromechanics: Relationship of Roughness to Closure and Wave Propagation, *International Journal of Geomechanics*, (in print) (2011).
[81] W. Noll, E.G. and Virga, On edge interactions and surface tension, *Arch. Rational Mech. Anal*., **111**(1), 1-31 (1990).
[82] M. Ouisse, J.-L. Guyader, Vibration Sensitive Behaviour of a connecting angle. Case of Coupled Beams and Plates, *J. Sound and Vibration* **267**, 809-850 (2003).
[83] C. Pideri, P. Seppecher, A second gradient material resulting from the homogenization of an heterogeneous linear elastic medium. *Contin. Mech. Thermodyn*. **9**(5), 241-257 (1997).
[84] C. Polizzotto, Strain-gradient elastic-plastic material models and assessment of the higher order boundary conditions. *Eur. J. Mech. A Solids* **26**(2), 189-211 (2007).
[85] G. Sciarra, F. dell'Isola, O. Coussy, Second gradient poromechanics. *Internat. J. Solids Structures* **44**(20), 6607-6629 (2007).
[86] G. Sciarra, F. dell'Isola, N. Ianiro and A. Madeo, A Variational Deduction of Second Gradient Poroelasticity I: General Theory, *J. Mech. Materials Struct*. **3**(3) 507-526 (2008).
[87] J. Salençon , Mécanique des milieux continus Ed. Ellipses (1988)-(1995) Handbook of Continuum Mechanics Ed. Springer, Berlin, (2001) Mécanique des milieux continus. Tome I. Éd. École polytechnique, Palaiseau ; Ellipses, Paris, (2002)-(2005)
[88] Seppecher, Etude d'une Modélisation des Zones Capillaires Fluides: Interfaces et Lignes de Contact. Thèse de l'Université Paris VI, Avril 1987
[89] P. Seppecher, Etude des conditions aux limites en théorie du second gradient: cas de la capillarité. *C. R. Acad. Sci. Paris*, t. **309**, Série II, 497-502 (1989).
[90] P. Seppecher, Equilibrium of a Cahn-Hilliard fluid on a wall: influence of the wetting properties of the fluid upon the stability of a thin liquid film. *European J. Mech. B Fluids* **12**(1), 69-84 (1993).
[91] M. Šilhavý, The existence of the flux vector and the divergence theorem for general Cauchy fluxes. *Arch.Ration. Mech. Anal*. **90** 195-211 (1985).
[92] M. Šilhavý, Cauchy's stress theorem and tensor fields with divergences in Lp. *Arch. Ration. Mech. Anal*. **116**, 223-255 (1991).
[93] M. Sokolowski, Theory of couple-stresses in bodies with constrained rotations. In *CISM courses and lectures*, **26**. Berlin, Germany: Springer (1970)
[94] P. Steinmann, E. A. Stein, Unifying Treatise of Variational Principles for Two Types of Micropolar Continua. Acta Mechanica 121(1-4), 215-232 (1997)
[95] R. Sunyk, P. Steinmann, On Higher Gradients in Continuum-Atomistic Modelling. Int. J. Solids Structures 40(24), 6877–6896 (2003)
[96] R.A. Toupin, Elastic materials with couple-stresses. *Arch. Rat. Mech. Anal*. **11**, 385-414 (1962).

[97] R.A. Toupin, Theories of elasticity with couple-stresses. *Arch. Rat. Mech. Anal.* **17**, 85-112 (1964).
[98] N.Triantafyllidis, E.C.A. Aifantis, Gradient approach to localization of deformation. I. Hyperelastic materials. *J. Elasticity* **16**(3), 225-237 (1986).
[99] N. Triantafyllidis, S. Bardenhagen, On higher order gradient continuum theories in 1-D nonlinear elasticity. Derivation from and comparison to the corresponding discrete models. *J. Elasticity*, **33** (1993).
[100] N. Triantafyllidis, S. Bardenhagen, The Influence of Scale Size on the Stability of Periodic Solids and the Role of Higher Order Gradient Continuum Models. *J. Mech. Phys. Solids* **44**(11), 1891-1928 (1996).
[101] Y. Yang, A. Misra, Higher-Order Stress-Strain Theory for Damage Modeling Implemented in an Element-free Galerkin Formulation. *CMES* **1549**(1), 1-36 (2010).
[102] Y. Yang , W.Y. Ching, A. Misra, Higher-order continuum theory applied to fracture simulation of nano-scale intergranular glassy film. Journal of Nanomechanics and Micromechanics, (in print) (2011)